Diffraction modelling for solar coronagraphy

Application to ASPIICS

Raphaël Rougeot

Laboratoire Lagrange, Nice – 12/02/2018

Outline

1) Proba-3 mission and ASPIICS
2) Diffraction from external occulters
3) Penumbra profile
4) Light propagation in the coronagraph
5) Conclusion

Proba-3 mission and ASPIICS

Proba-3 mission

- In-orbit demonstration of precise **Formation Flying**
- Two spacecraft flying **144m apart**, controlled with a millimeter accuracy
- The Occulter Spacecraft will carry a 1,42m diameter occulter disk
- The Coronagraph Spacecraft will fly the solar coronagraph

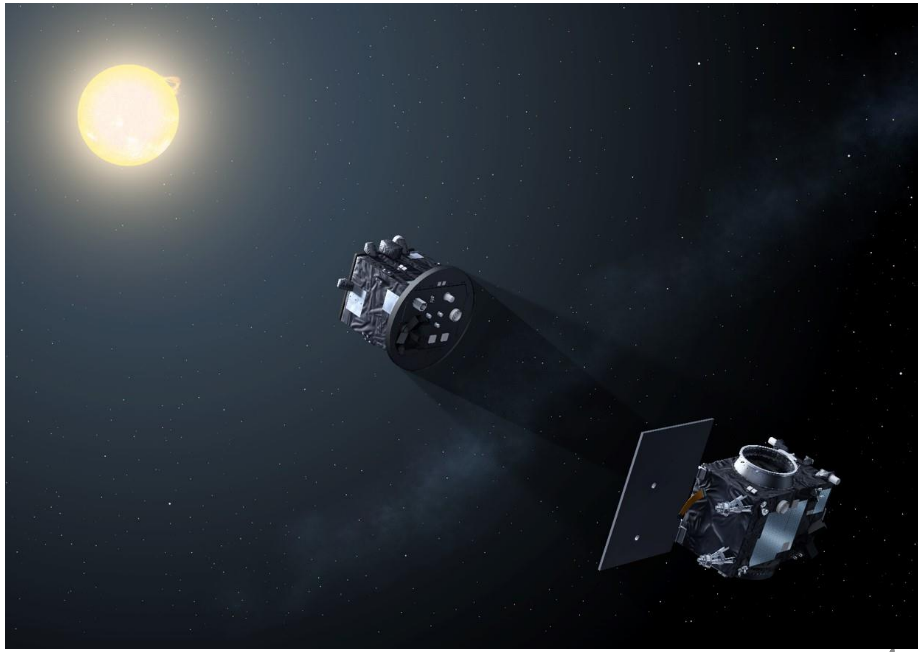

Proba-3 mission

- The formation will be **co-aligned with the Sun** during the **6-hours** apogee phase

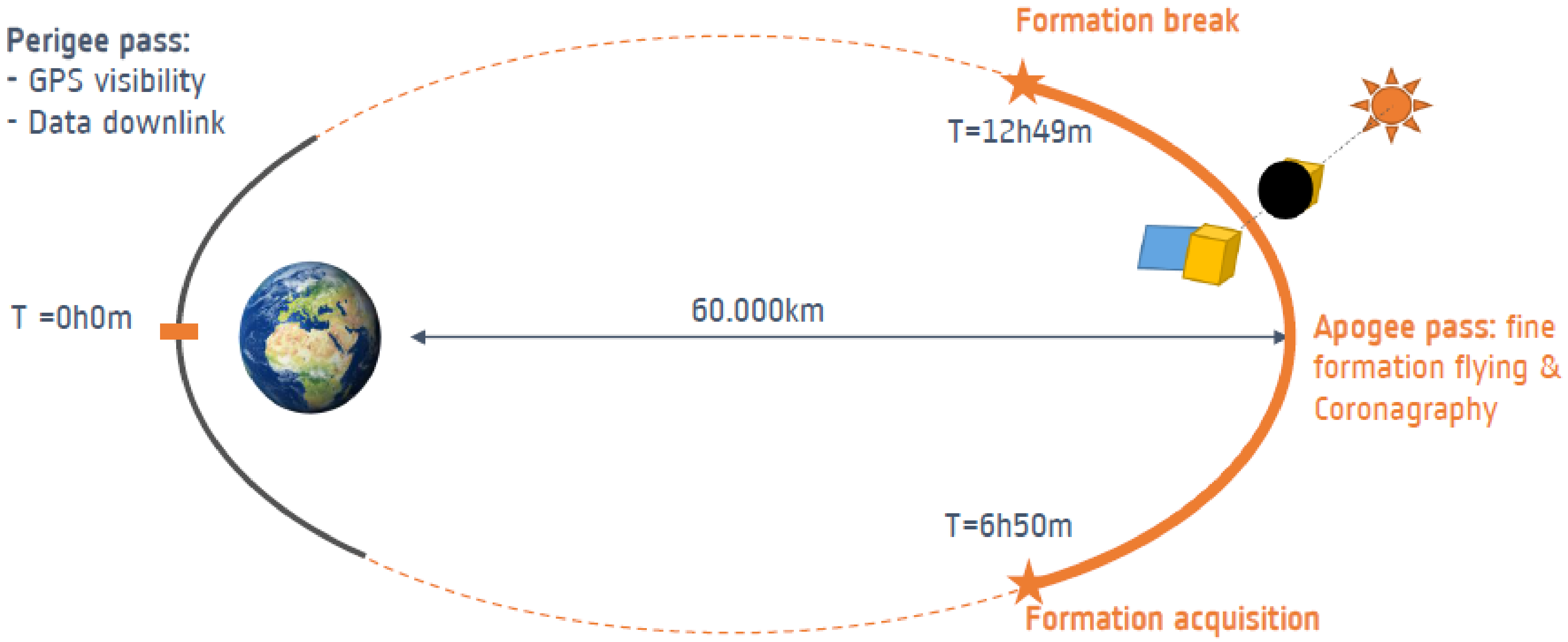

Solar coronagraph ASPIICS

- Associtation de Satellites Pour l'Imagerie et l'Interférométrie de la Couronne Solaire

- ASPIICS in a nutshell:
  - white light [540nm ; 570nm]
  - 2,81 arcsec/pixel
  - 3 polarizers
  - high cadence

- Observation of the K-corona:
  - Findings on the heating process
  - Alven's waves, dynamics of the plasma
  - Coronal Mass Ejections

Solar coronagraph ASPIICS

- Hybrid externally occulted Lyot-style solar coronagraph

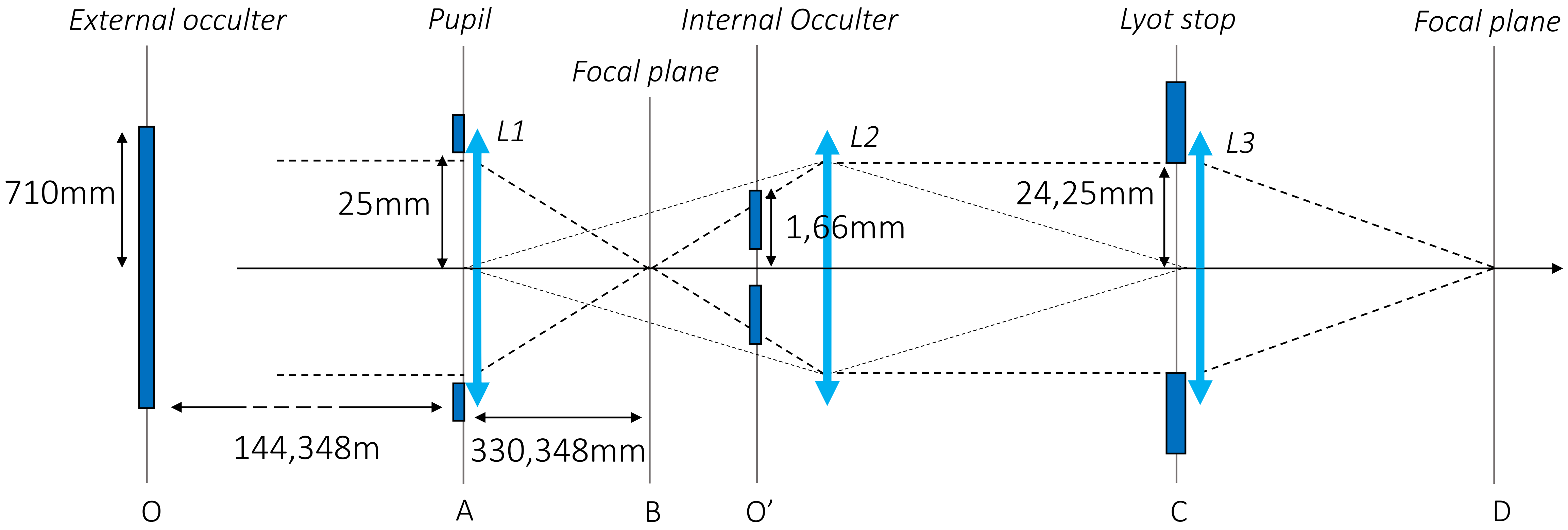

Diffraction by an external occulter

Diffraction by an external occulter

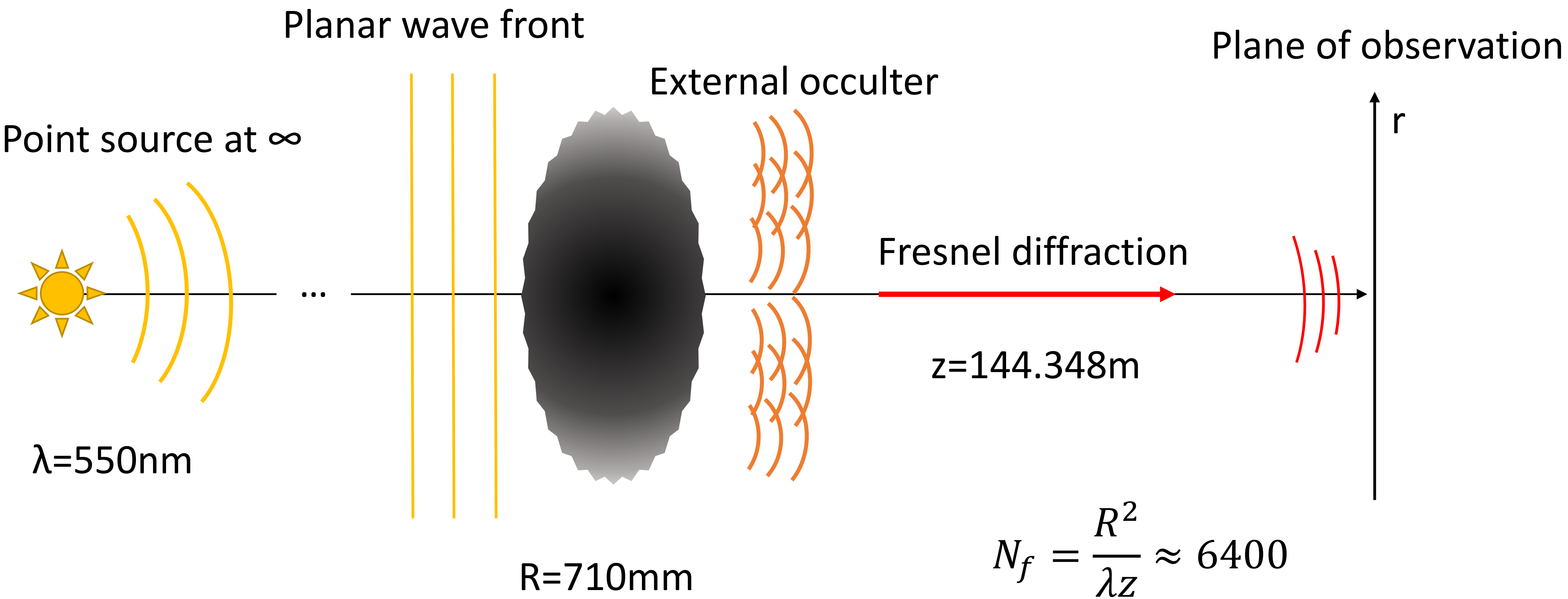

$$N_f = \frac{R^2}{\lambda z} \approx 6400$$

Diffraction by an external occulter

Major point in solar coronagraphy: the Sun is an extended source!

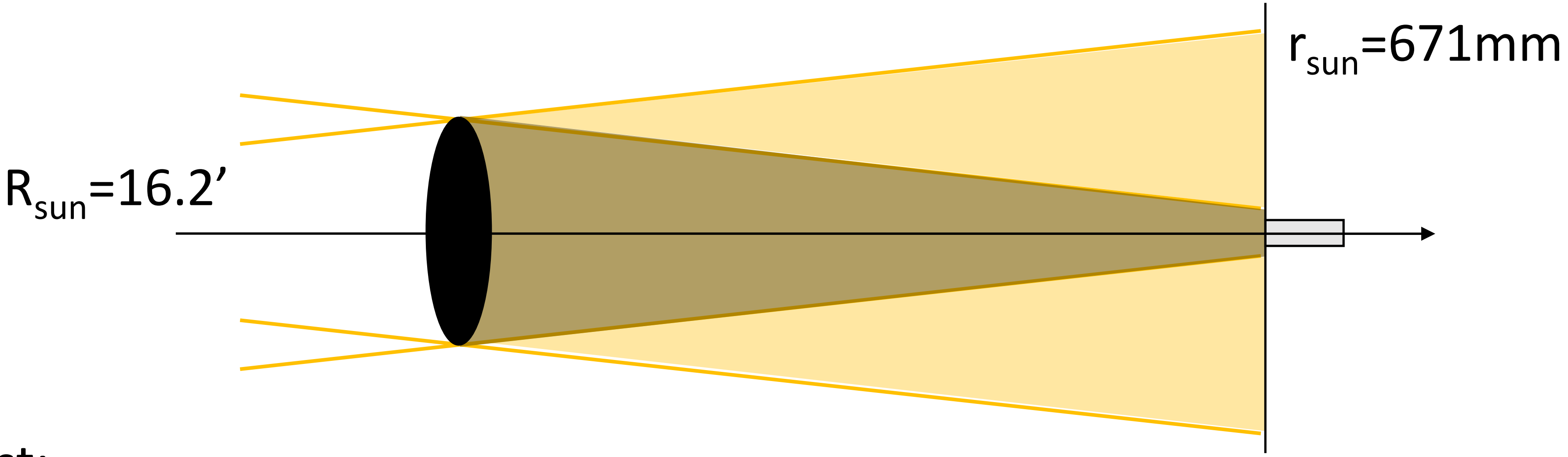

We must:
- know the diffraction pattern over a large extent
- perform a convolution with the solar disk
- what happens in the centre (few λ/D) is not sufficient!

≠ stellar coronagraphy

Diffraction by an external occulter

We investigated several numerical methods to compute diffraction (solar case):

- Analytical Hankel transformation:
  - \+ Exact calculation
  - \- Axis-symmetry required (only radial apodisation), computational time
- Brute force 2D FFT to compute the two dimension Fresnel integrals:
  - \+ Any type of occulters
  - \- Strong sampling requirements, very large size of arrays (order 10^5 to 10^6)
- Vanderbei et al. (2007) approach:
  - \+ Expands the Fresnel integral into a series
  - \- Not suitable for our solar case
- Maggi-Rubinowicz representation, the boundary diffraction integral:
  - \+ Fast and accurate
  - \- Requires a 1-or-0 occulter (no apodization)

Diffraction by an external occulter

- The sharp-edged occulting disk

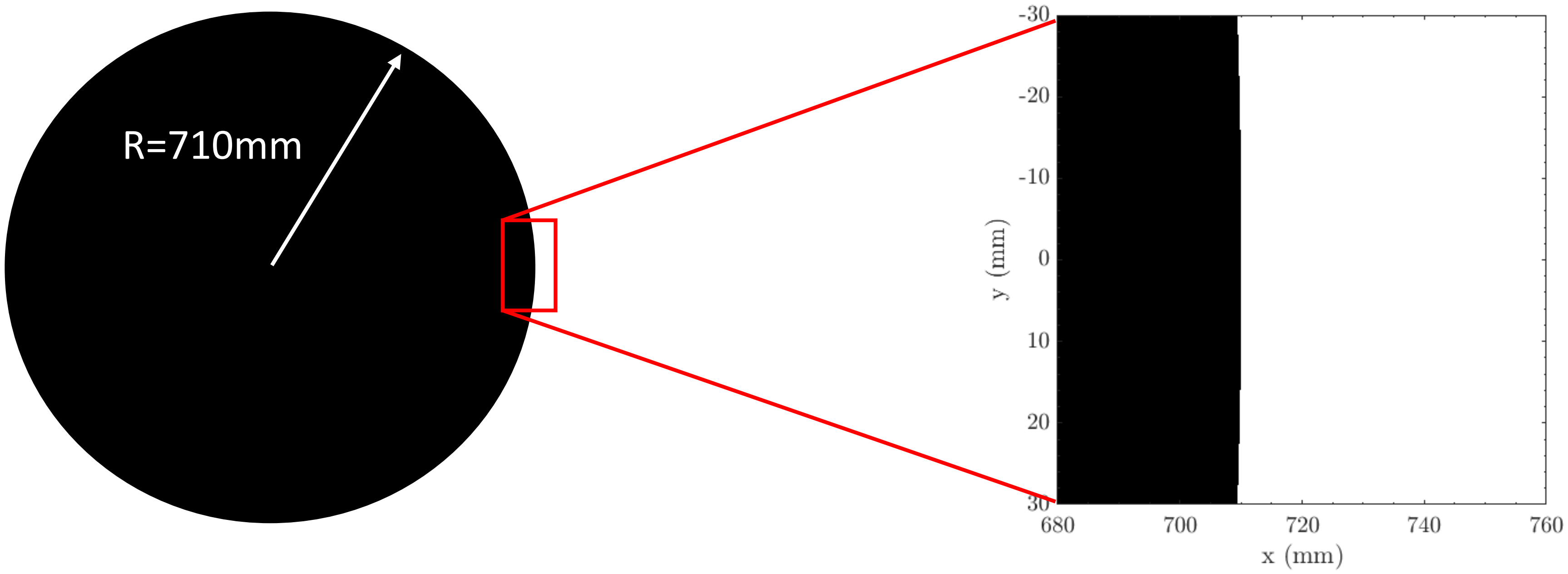

Occulting ratio of 1,05 solar radius at z_0=144m

Diffraction by an external occulter

- The sharp-edged occulting disk

The bright spot of Arago (or Poisson… demonstrated by Fresnel)

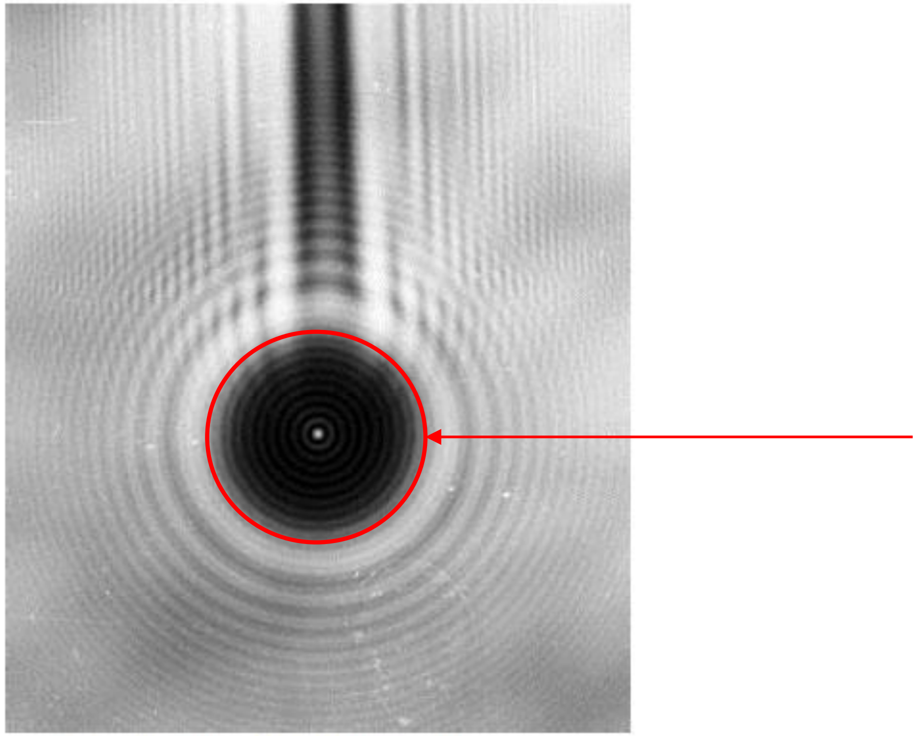

Geometrical umbra

Credit: Minerva.union.edu

Diffraction by an external occulter

- The sharp-edged occulting disk

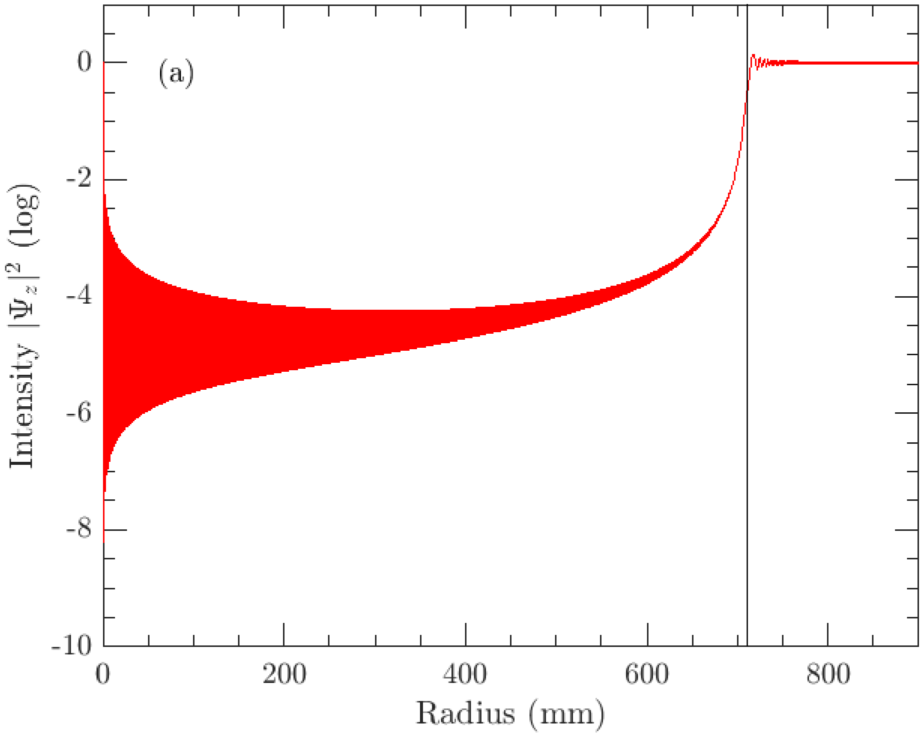

Bright spot of Arago

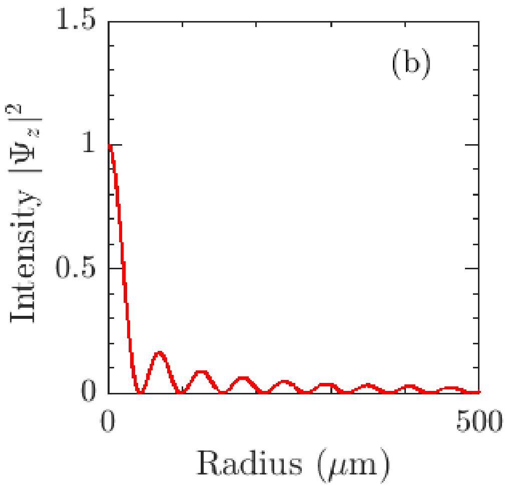

Transition shadow/light

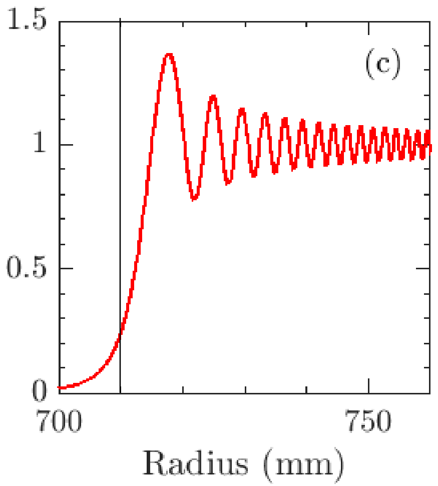

Diffraction by an external occulter

- The apodized occulting disk

Variable radial transmission

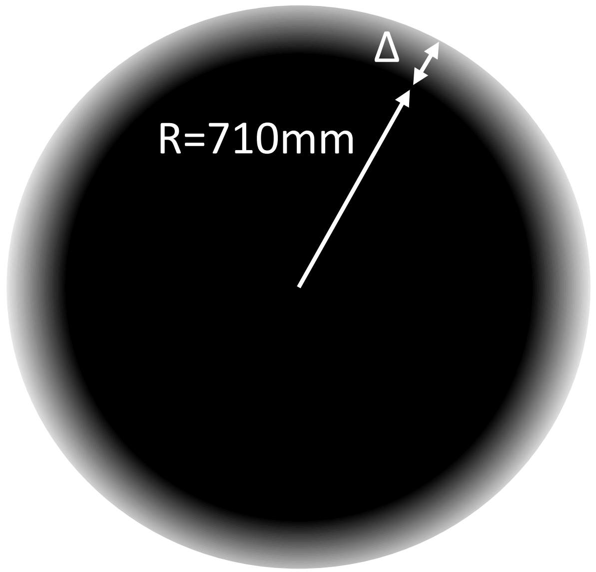

Diffraction by an external occulter

- The apodized occulting disk

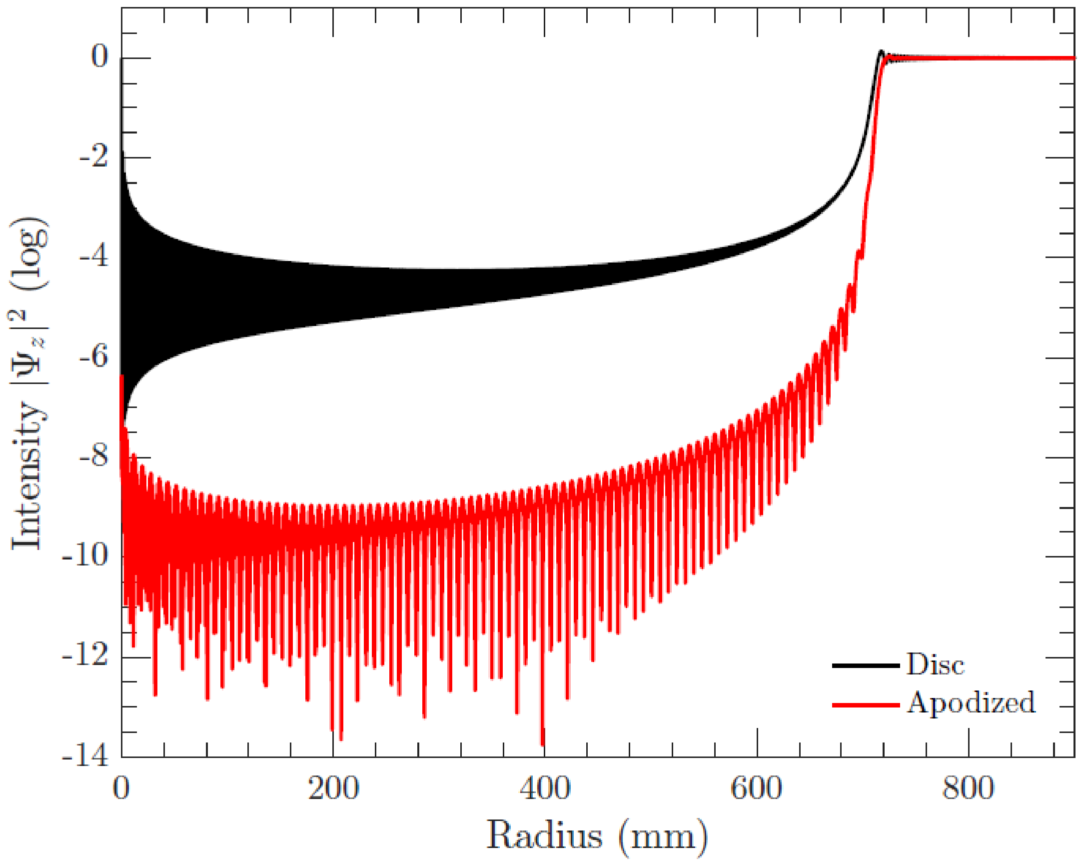

Diffraction by an external occulter

- The serrated (or petalized) occulter

  In stellar coronagraphy, the reasoning starts from the ideal apodized occulter

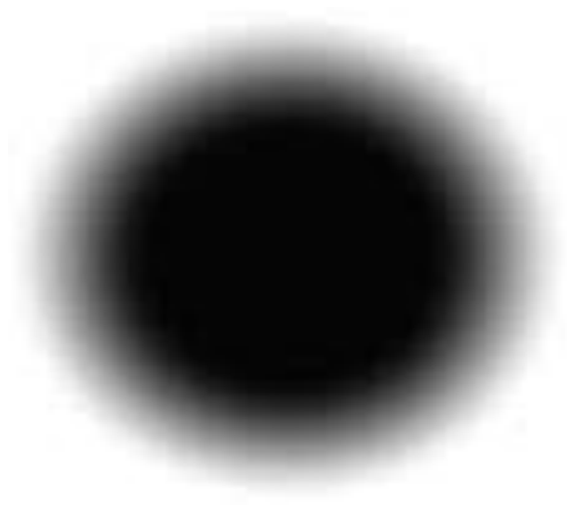

$$\tau_{apod}(r) = \int \tau_{petal}(r,\theta)d\theta$$

Cady, 2006
Vanderbei et al., 2007

The petalized occulter is the discrete substitute

Diffraction by an external occulter

- The serrated (or saw-toothed) occulter

  In solar coronagraphy, the reasonning is well different!

  The diffraction occurs perpendicularly to the edge
  A toothed disc rejects the light outside the central region

  Boivin (1978) predicted the radius of the dark inner region of the diffraction pattern based on geometrical considerations

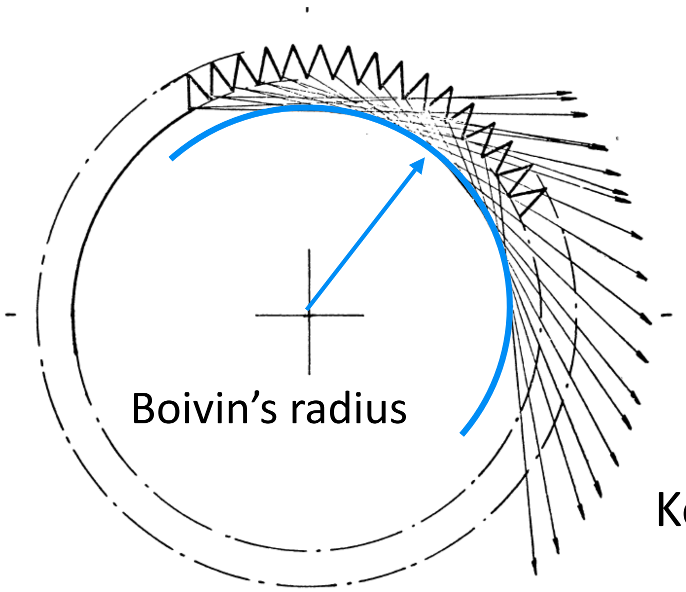

Koutchmy, 1988

Diffraction by an external occulter

- The serrated (or saw-toothed) occulter

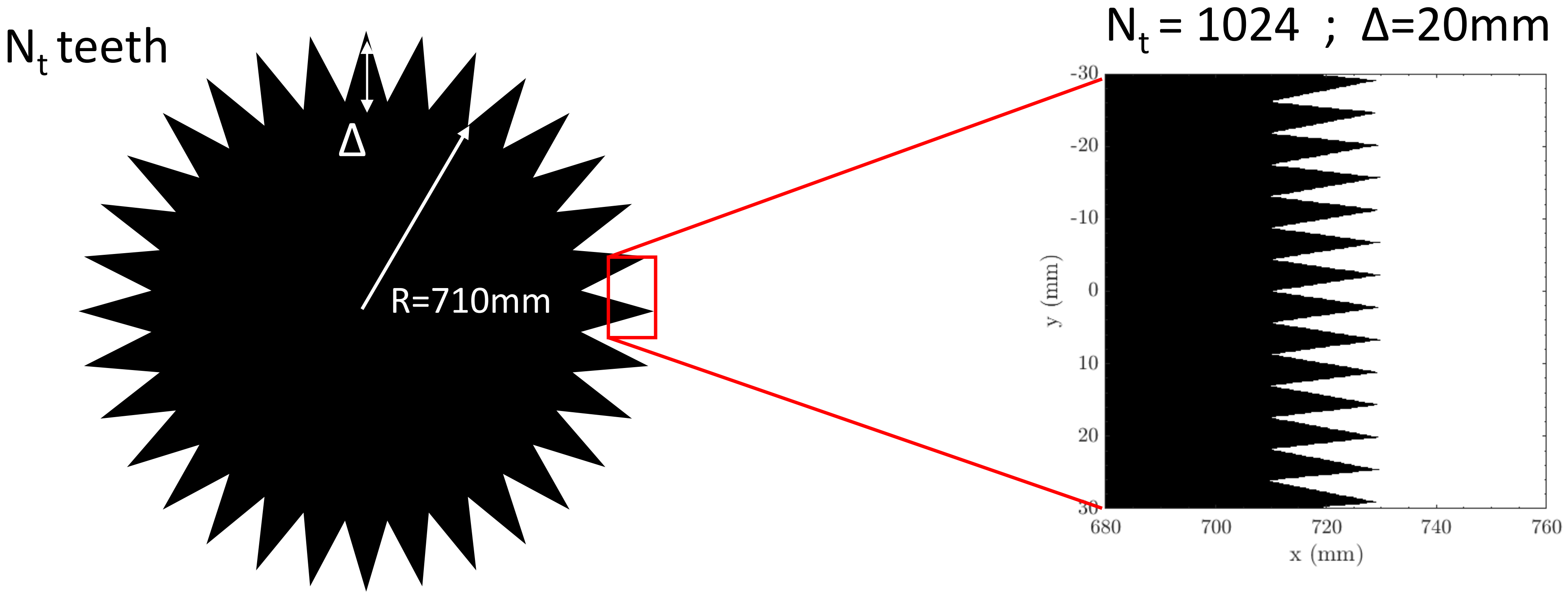

Diffraction by an external occulter

- The serrated (or saw-toothed) occulter

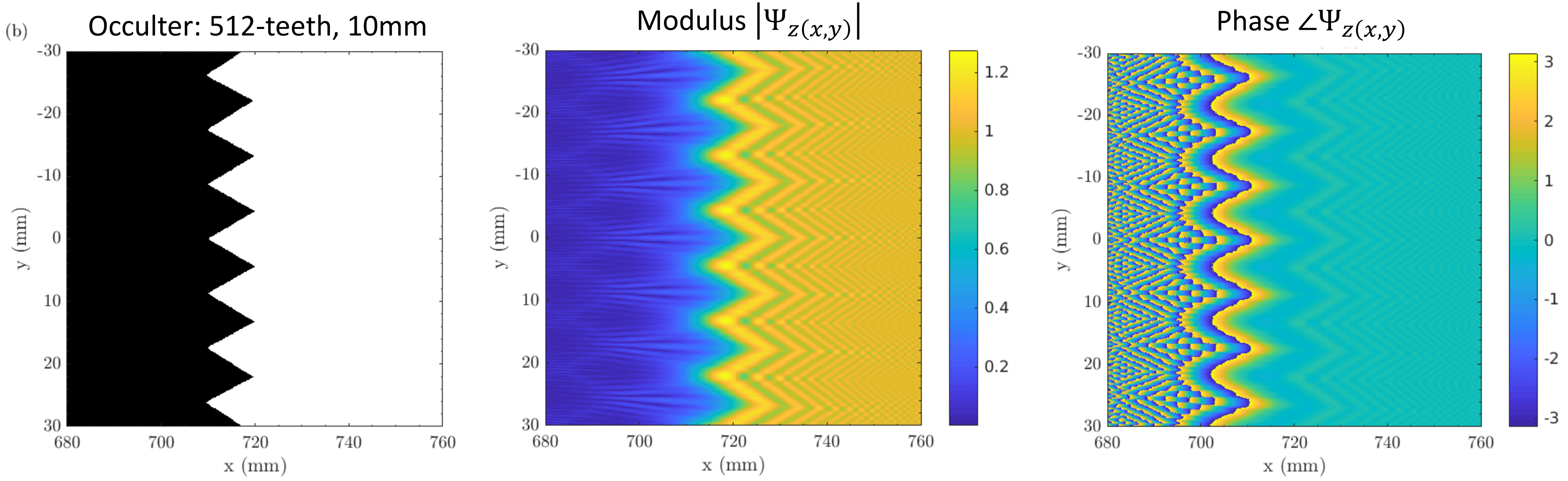

Diffraction by an external occulter

- The serrated (or saw-toothed) occulter

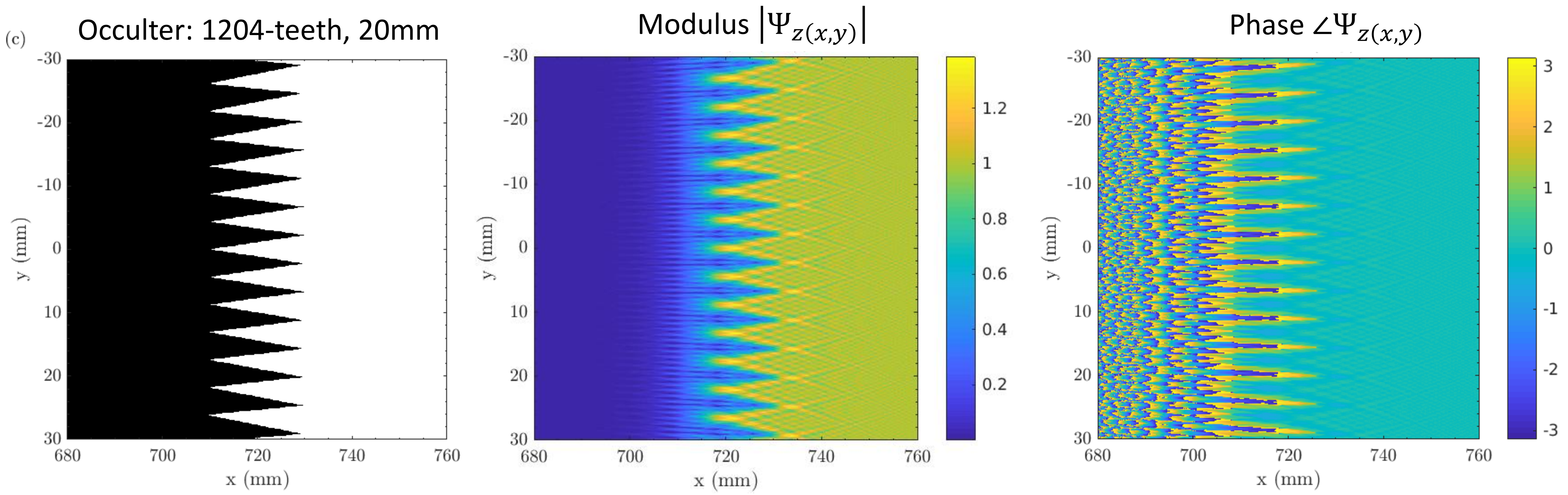

Diffraction by an external occulter

- The serrated (or saw-toothed) occulter

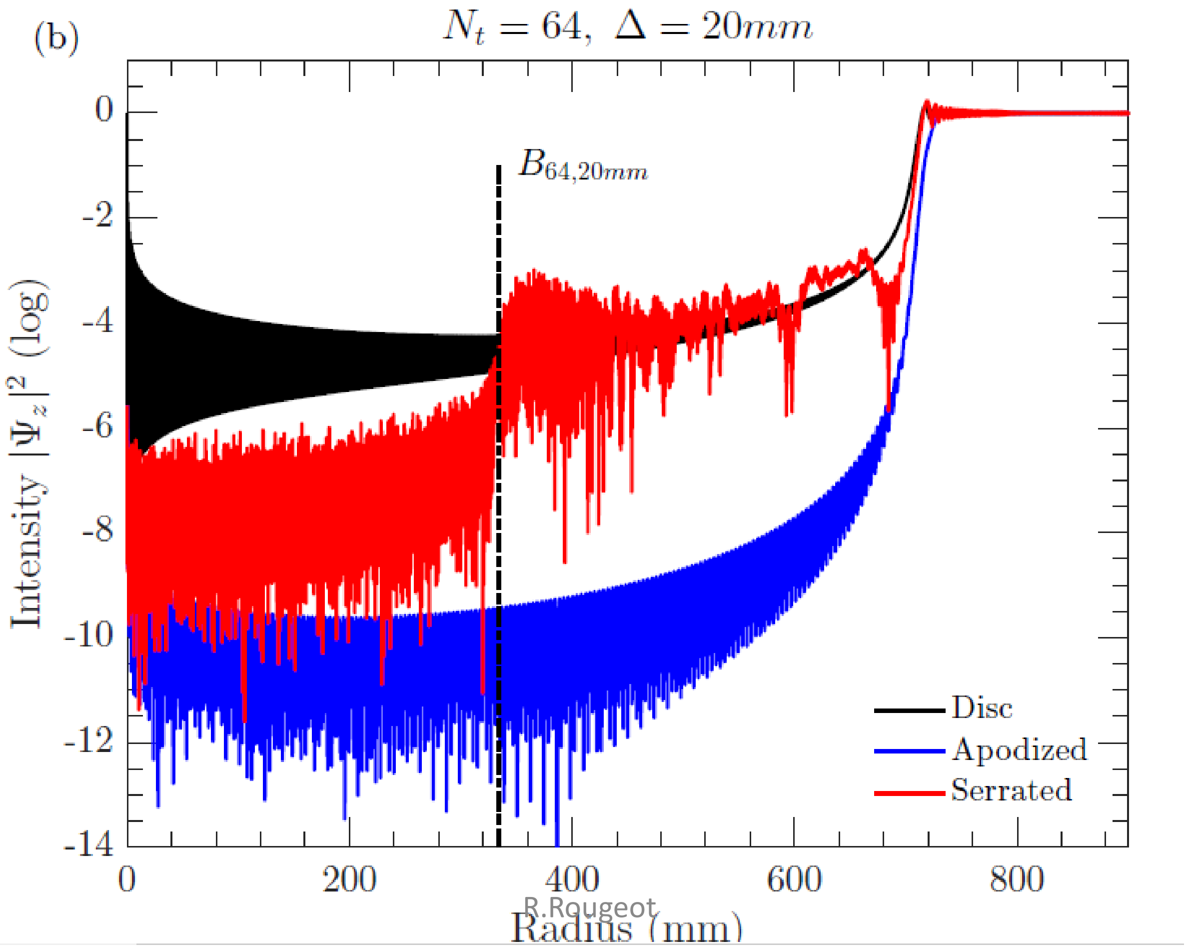

Diffraction by an external occulter

- The serrated (or saw-toothed) occulter

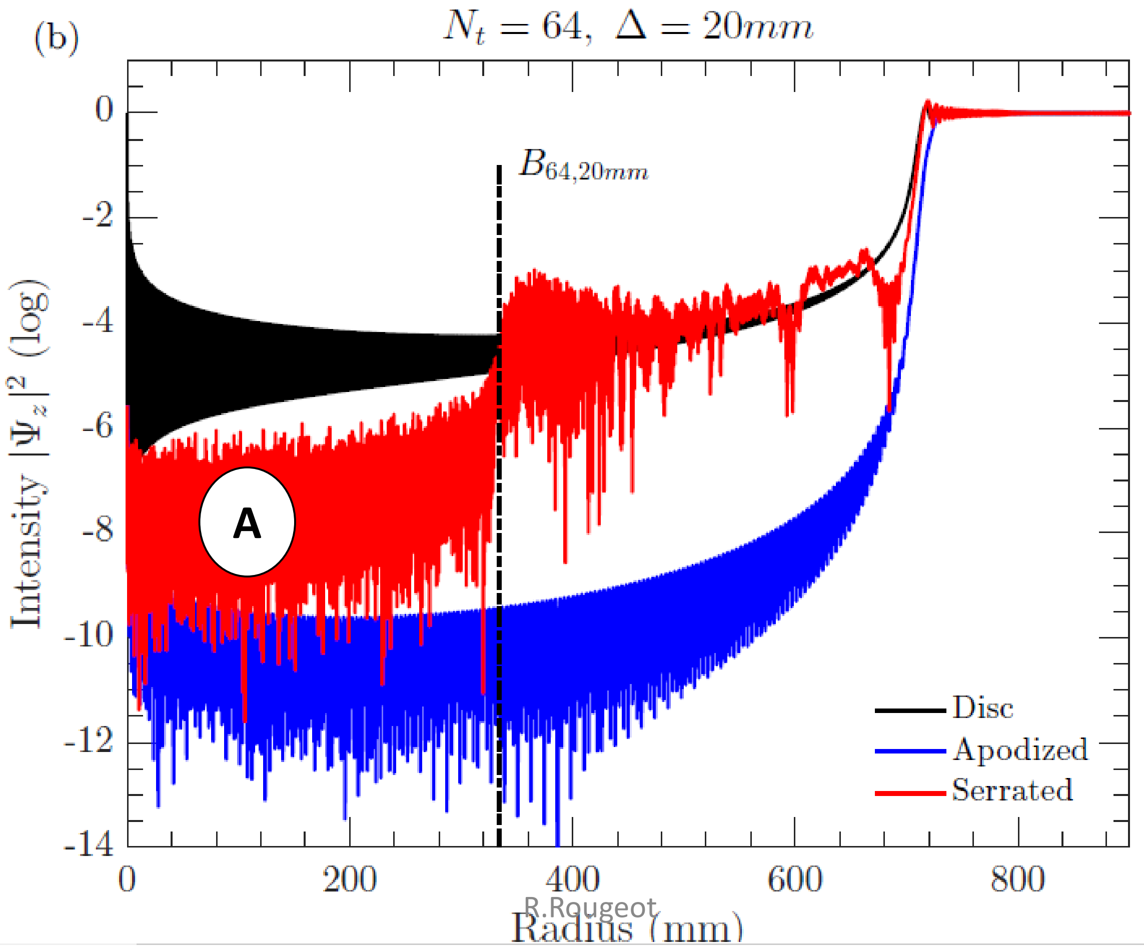

A Dark inner region

Diffraction by an external occulter

- The serrated (or saw-toothed) occulter

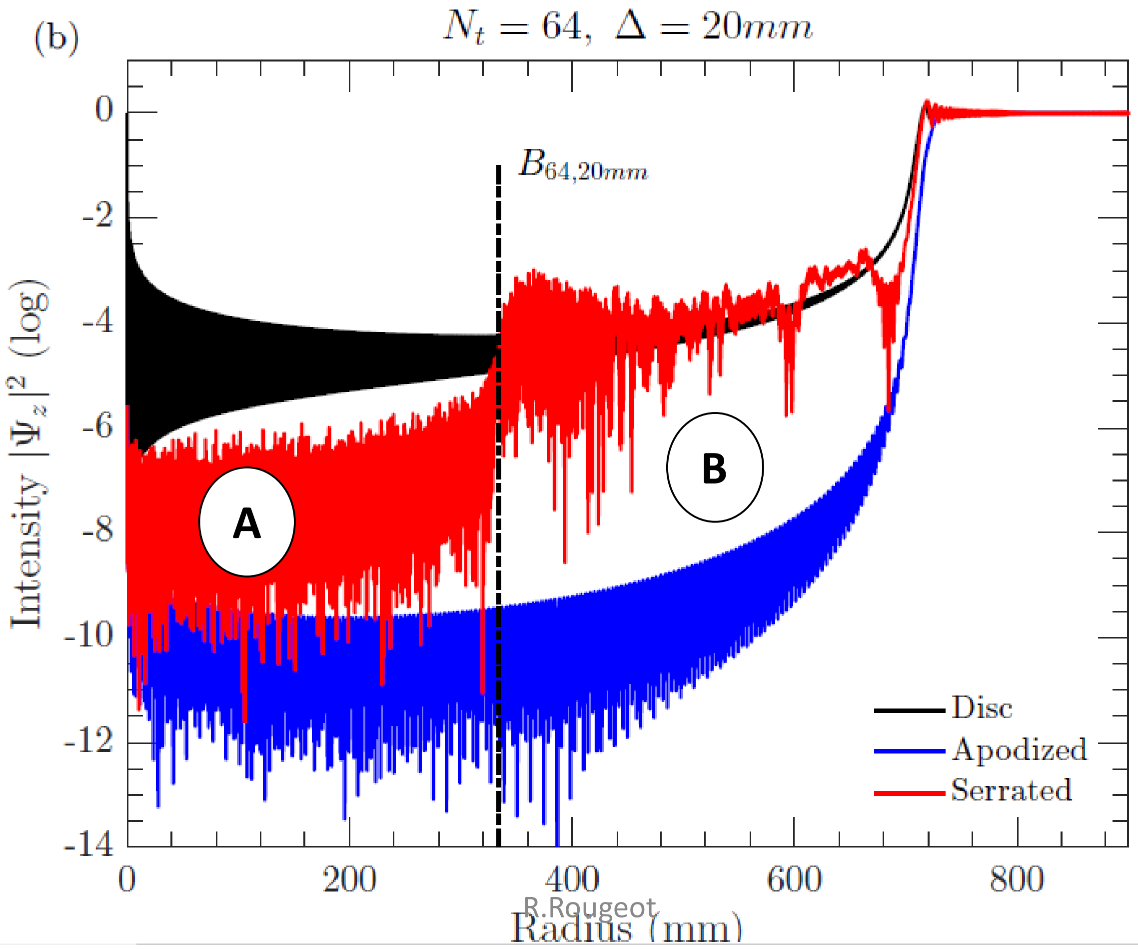

A Dark inner region

B Intermediate region

Diffraction by an external occulter

- The serrated (or saw-toothed) occulter

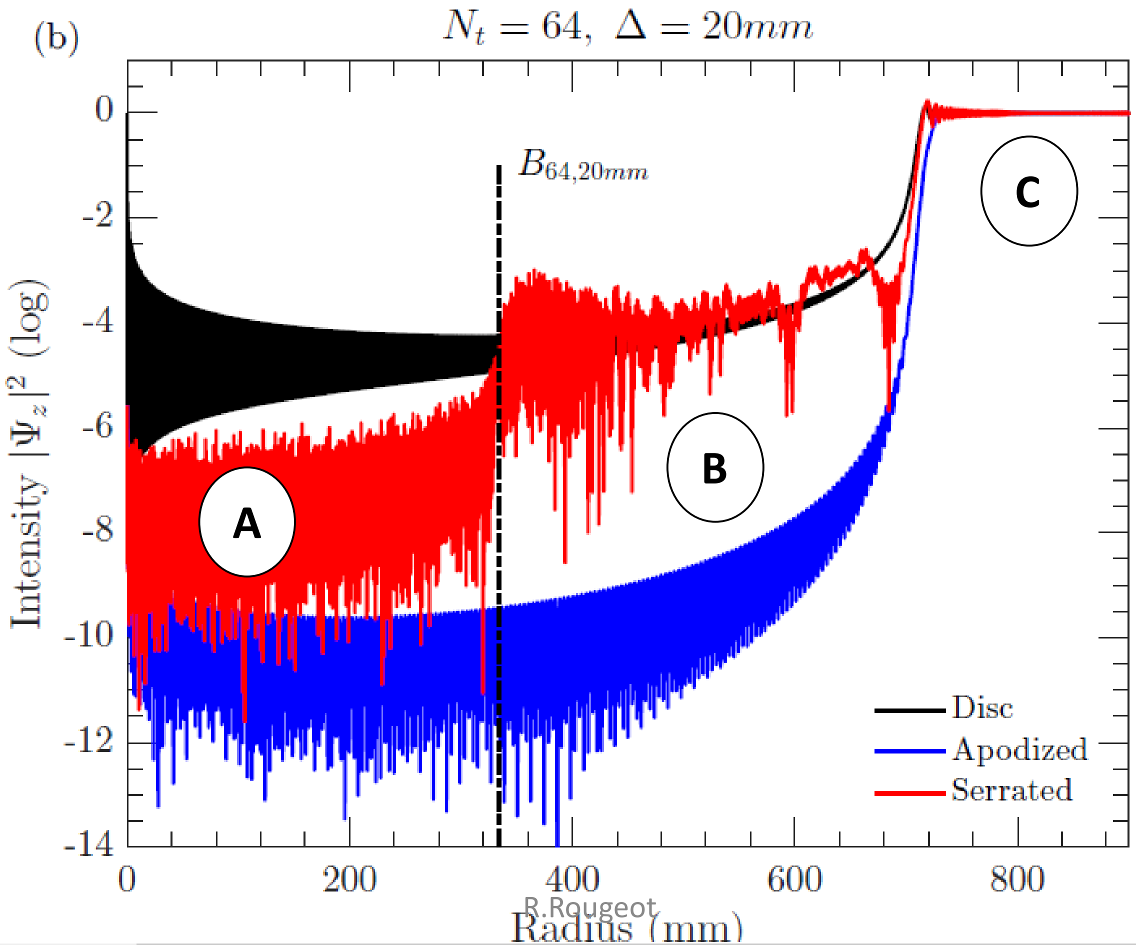

A Dark inner region

B Intermediate region

C Fully illuminated region

Diffraction by an external occulter

- We numerically verified the geometrial predictions of Boivin (1978)

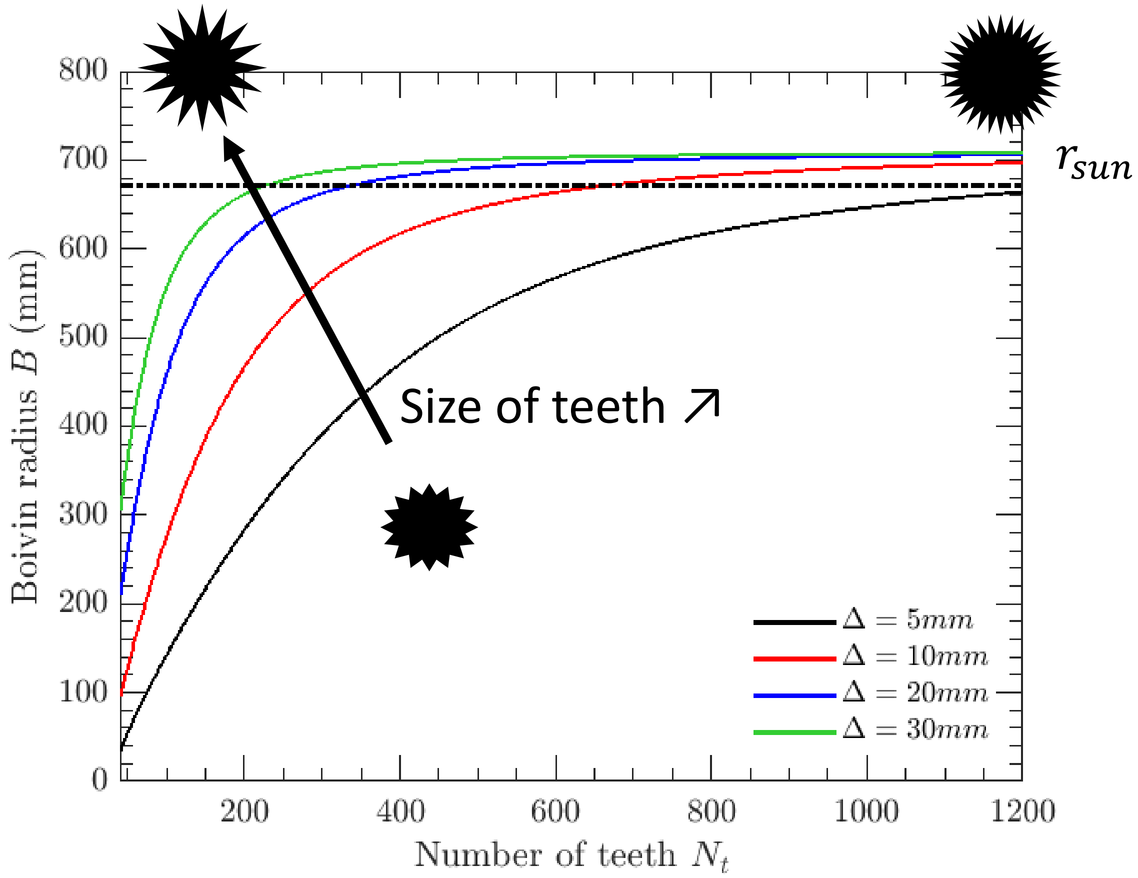

Diffraction by an external occulter

- The serrated (or saw-toothed) occulter

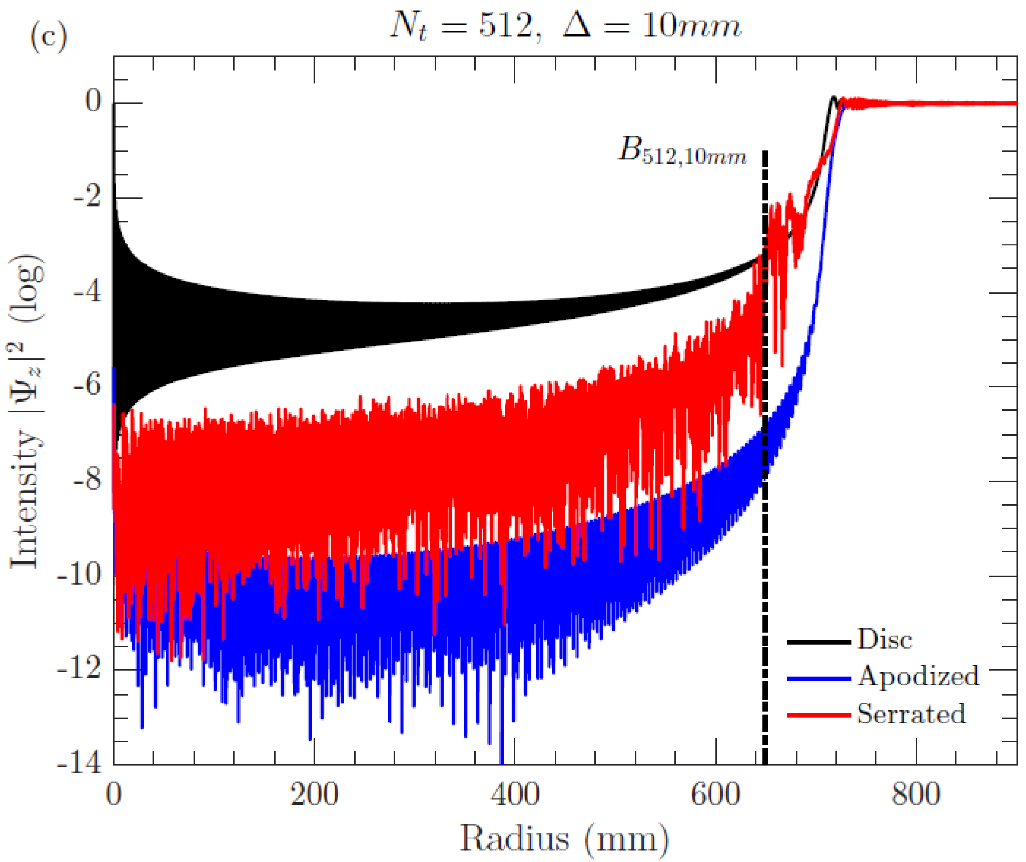

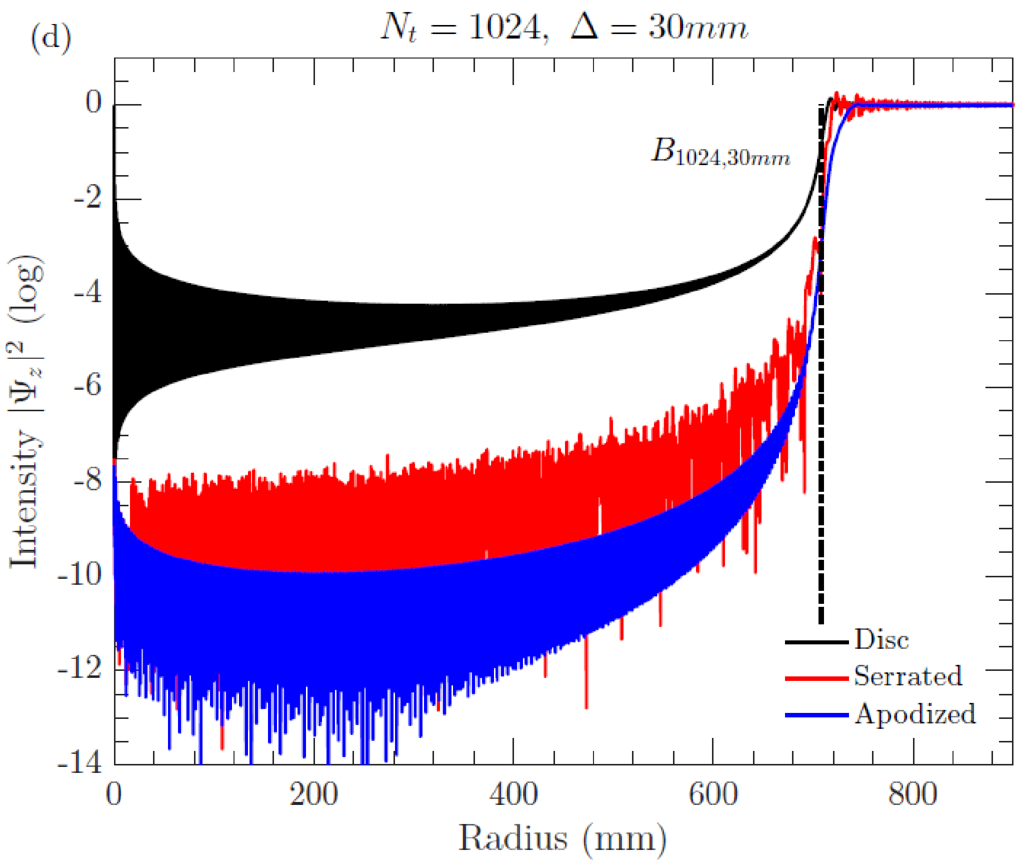

Penumbra profiles

Penumbra profiles

Major point in solar coronagraphy: the Sun is an extended source!

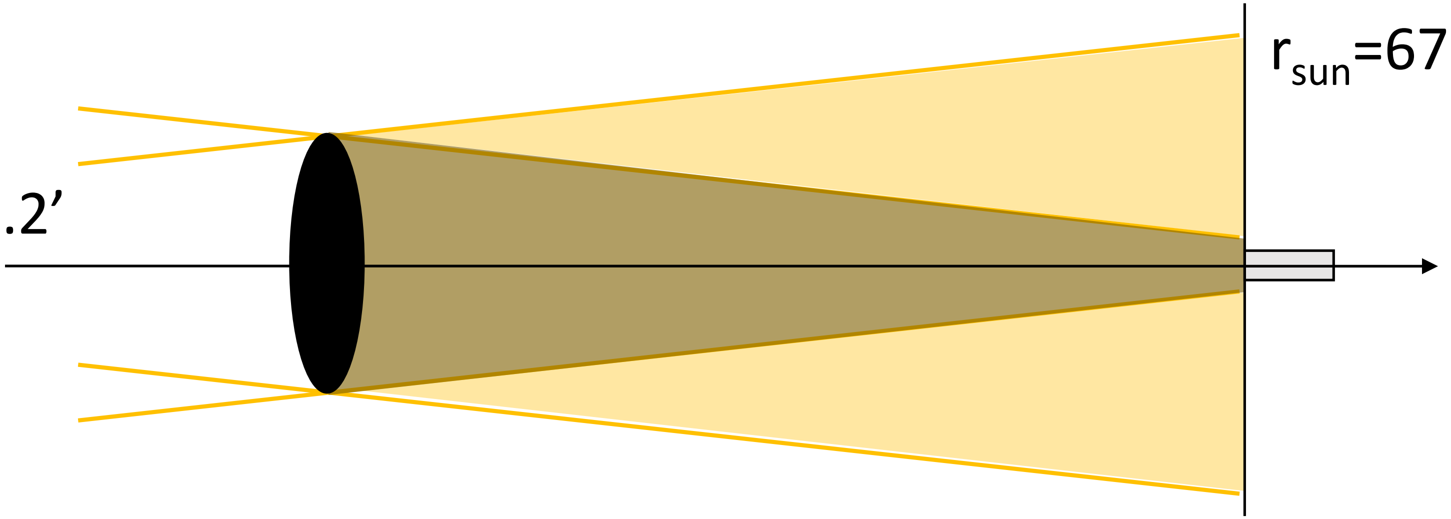

To compute the penumbra, we must:
- know the diffraction pattern over a large extent
- perform a convolution with the solar disk

Penumbra profiles

Major point in solar coronagraphy: the Sun is an extended source!

R_{sun}=16.2’

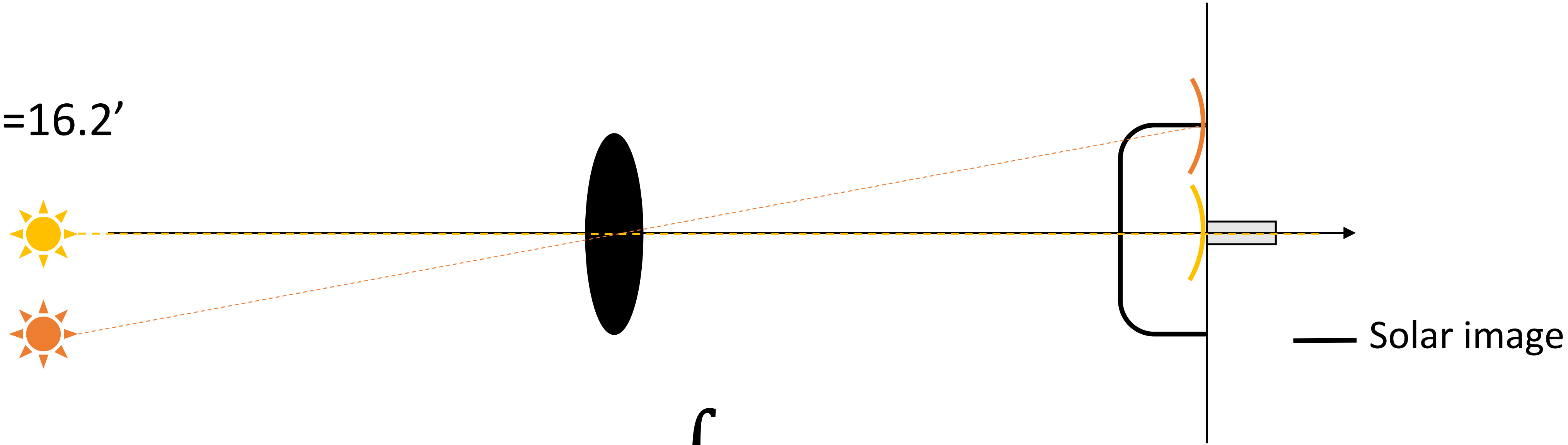

Penumbra: $\int_{\odot}$ Diffraction x Solar image

Penumbra profiles

- The sharp-edged occulting disk

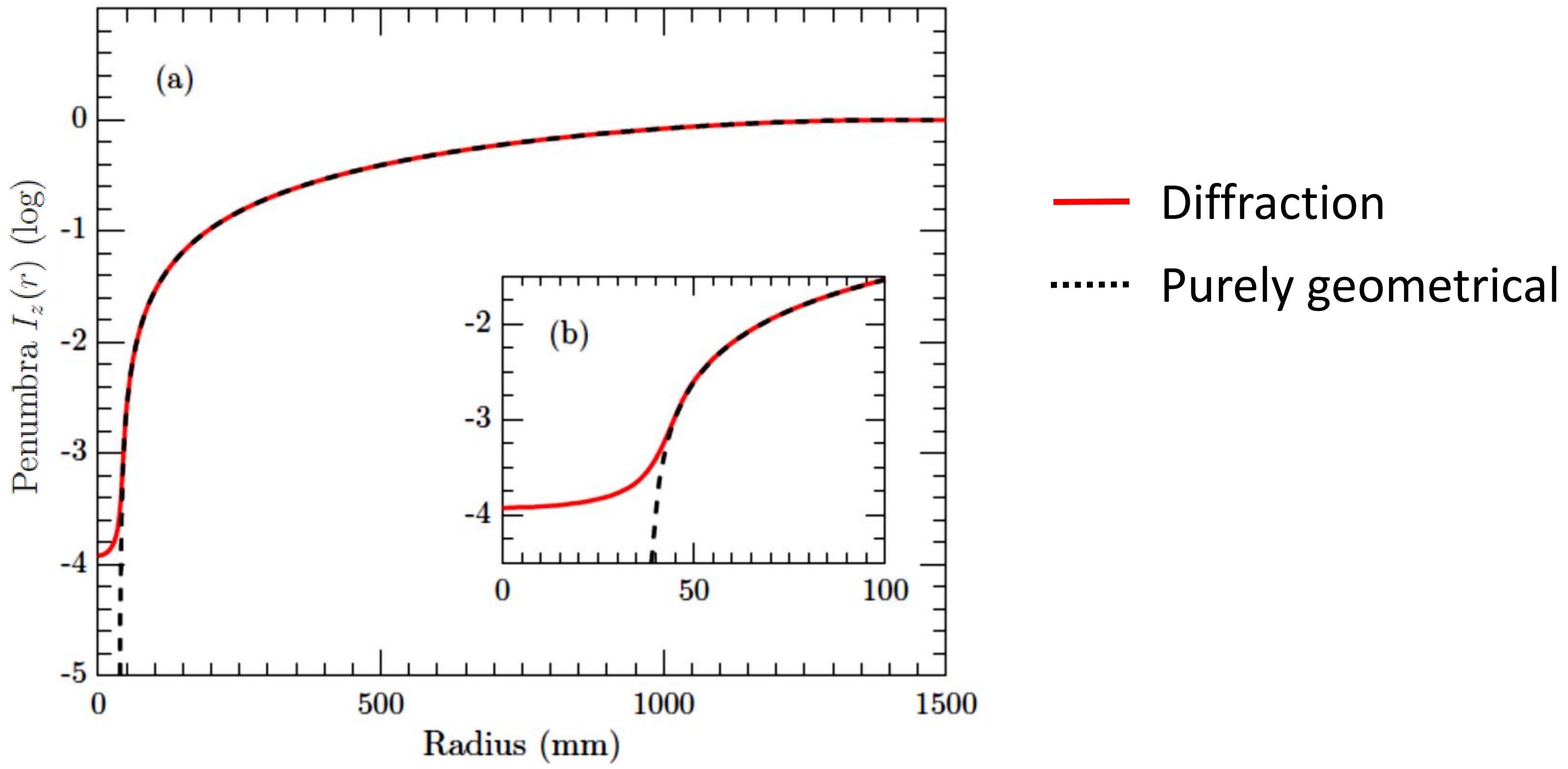

Penumbra profiles

- The serrated (or saw-toothed) occulter

Δ=20mm

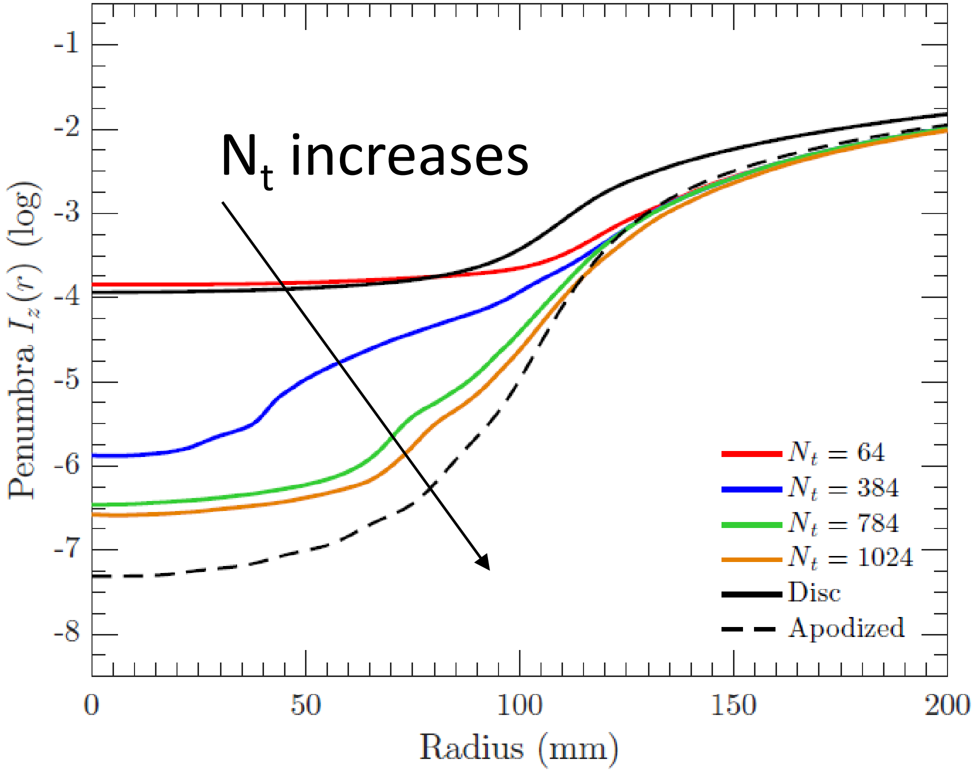

N_t=464

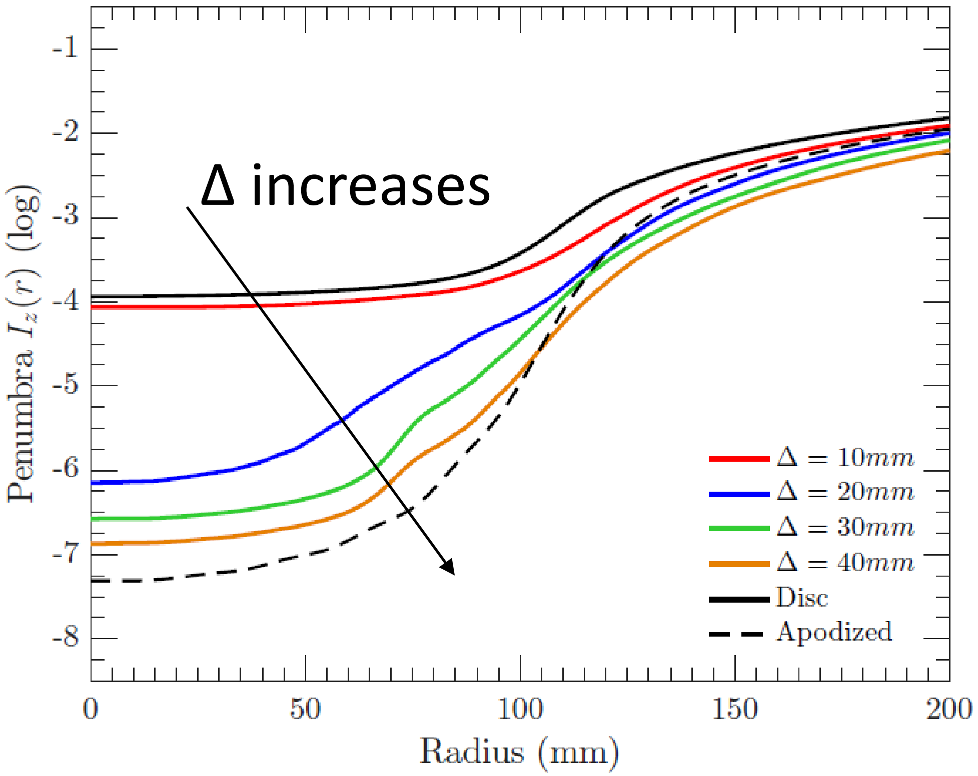

Penumbra profiles

- The serrated (or saw-toothed) occulter

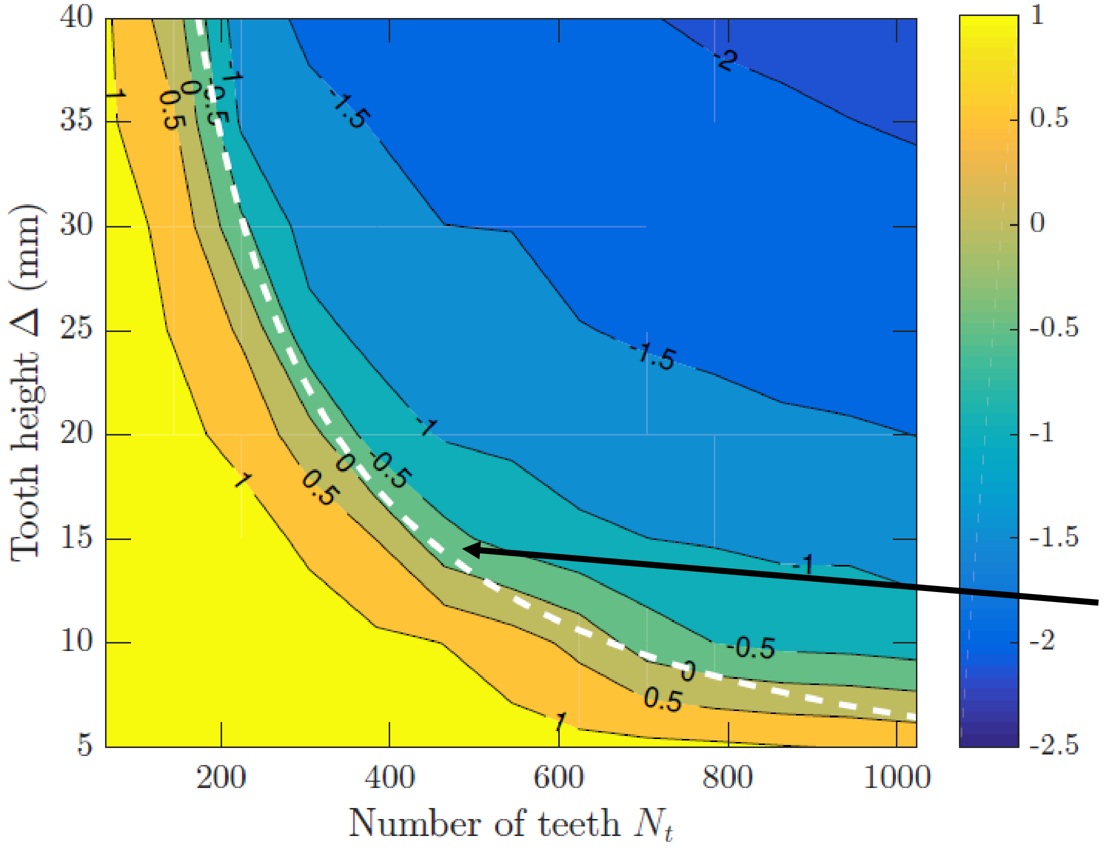

Integrated illumination over the pupil, normalized to the sharp-edged disk case

Boivin radius$(N_t, \Delta) > r_{sun}$ =671mm

Propagation inside the coronagraph

Propagation inside the coronagraph

- The hybrid externally occulted Lyot solar coronagraph

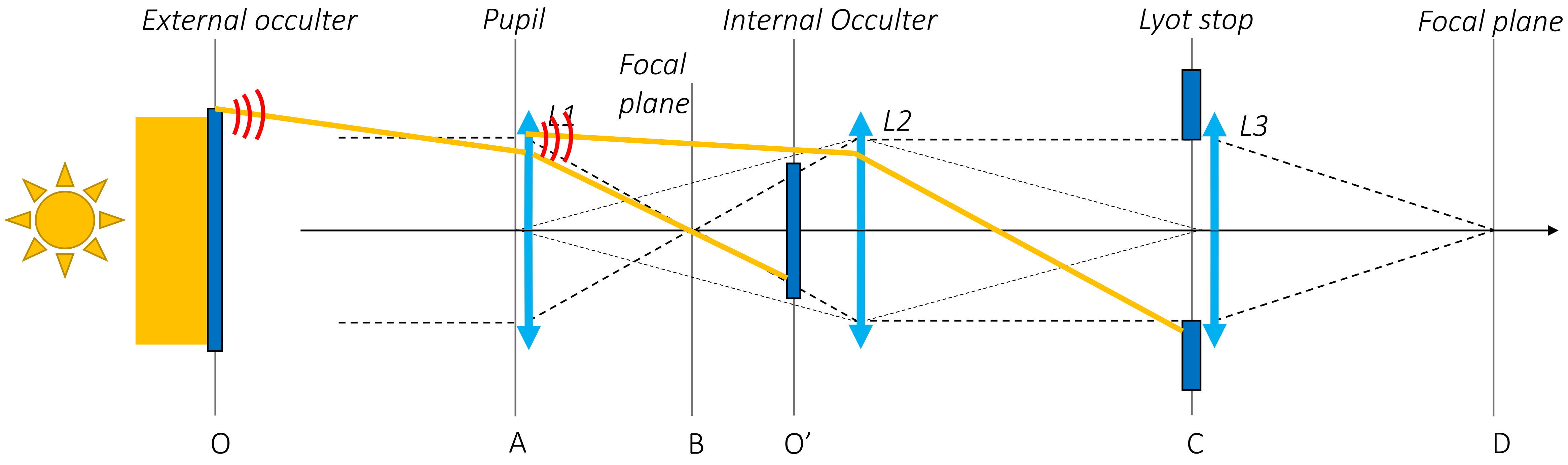

Propagation inside the coronagraph

- Propagation of the diffracted wave front from one plane to the next one
  - Fourier optics formalism, Fresnel free-space propagation
  - Ideal optics
  - Perfect axis-symetric geometry
- Integration over the solar disk
- Numerical implementation: successive FFT2 with arrays of large size
- Objective:
  - estimate the level and spatial distribution of the residual diffracted sunlight
  - address the rejection performance of the coronagraph

Propagation inside the coronagraph

- Intensity in plane O’, with the internal occulter

Without external occulter

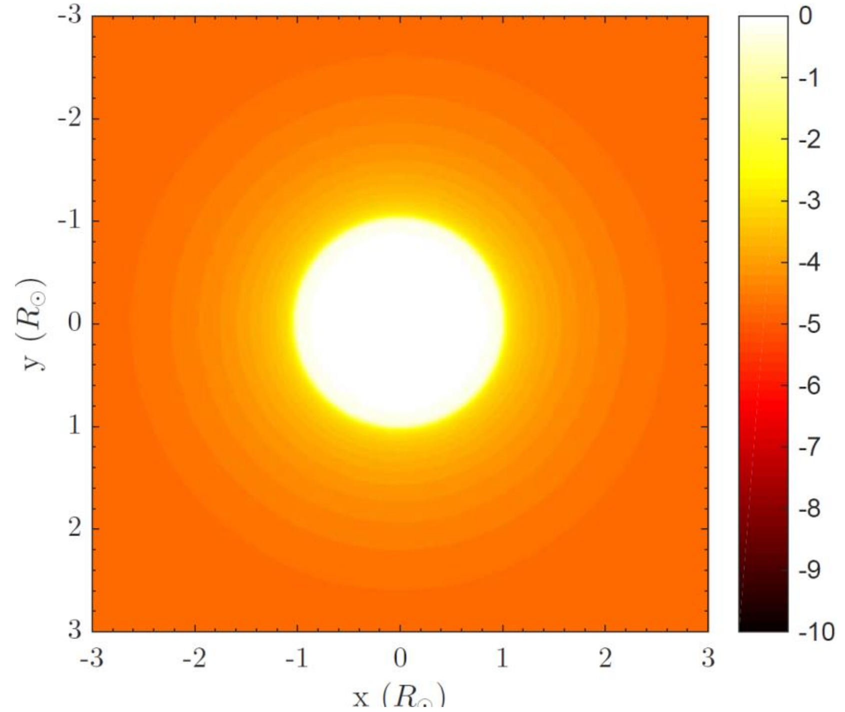

With external occulter

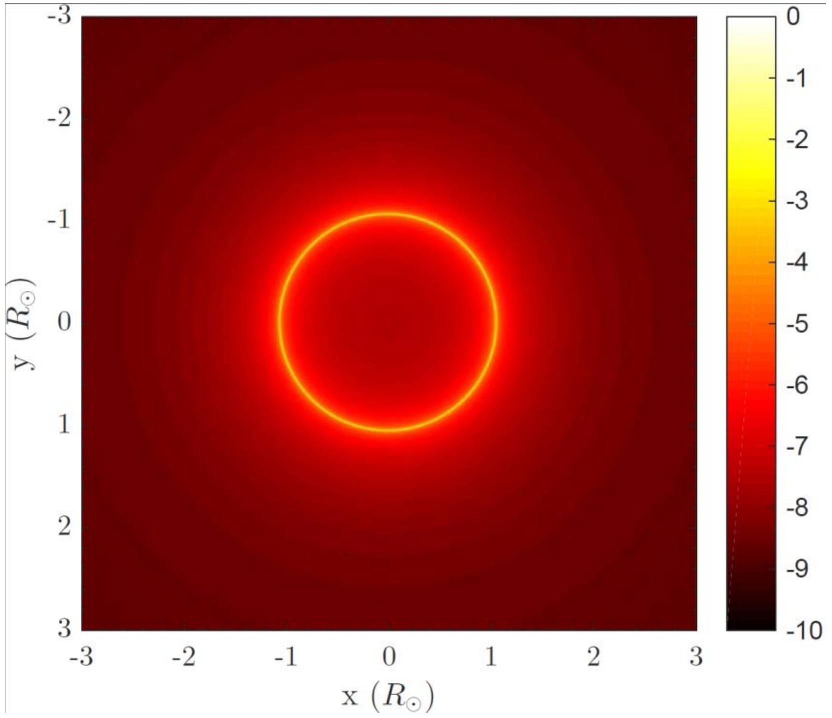

Propagation inside the coronagraph

- Intensity in plane O', with the internal occulter

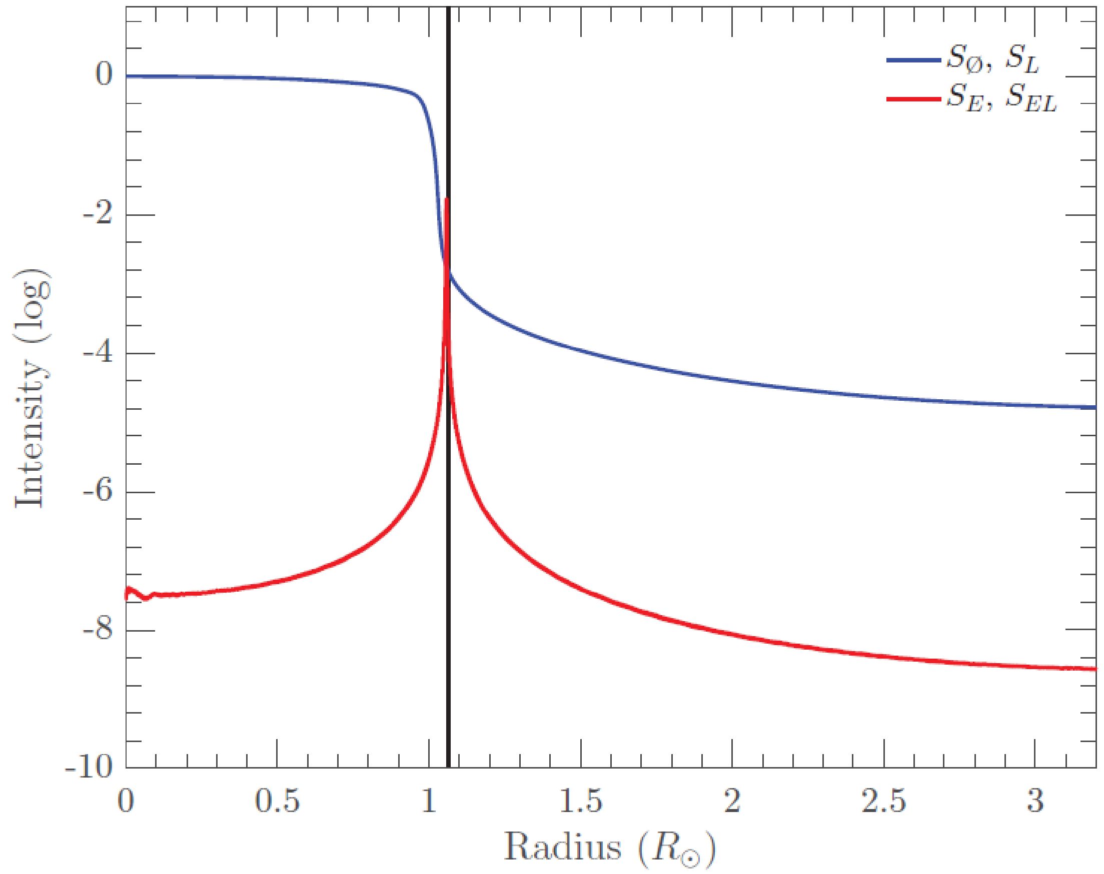

With external occulter

Without external occulter

Solar disk image (out-of-focused)

Propagation inside the coronagraph

- Intensity in plane O', with the internal occulter

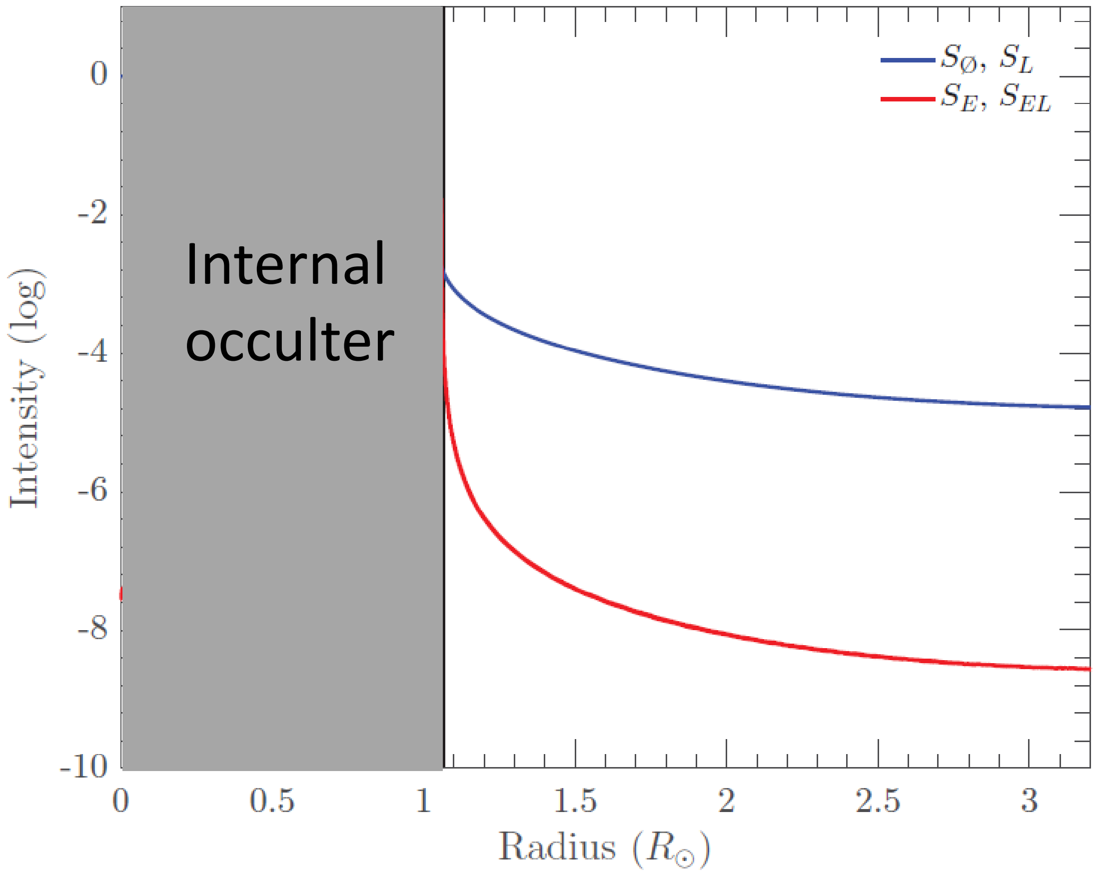

With external occulter

Without external occulter
Solar disk image (out-of-focused)

Propagation inside the coronagraph

- Intensity in plane C, with the Lyot stop

Without external occulter

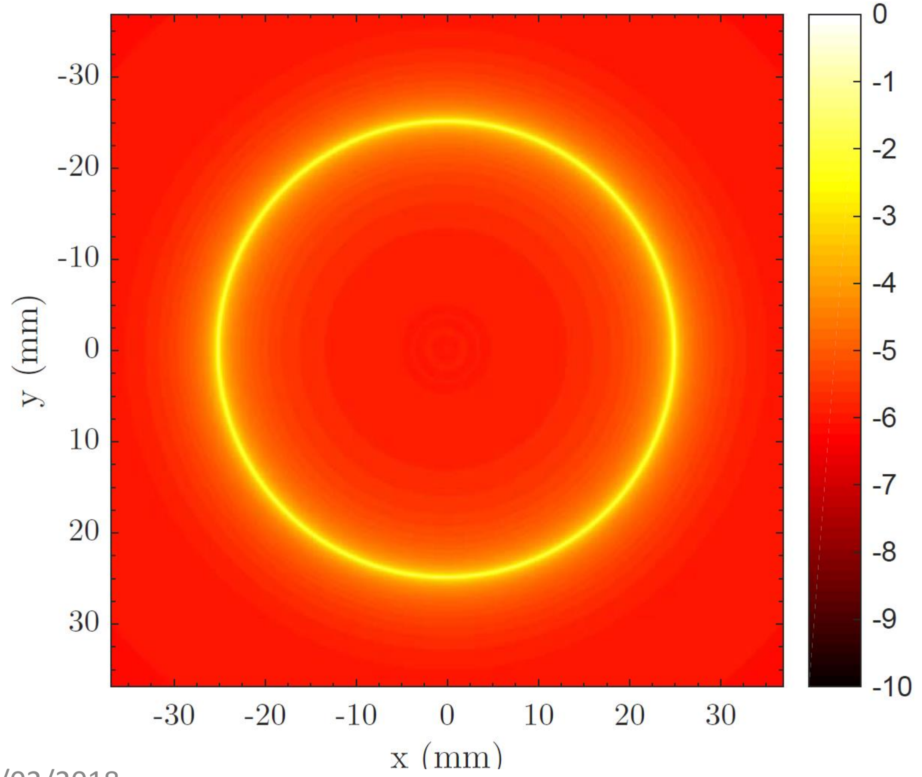

With external occulter

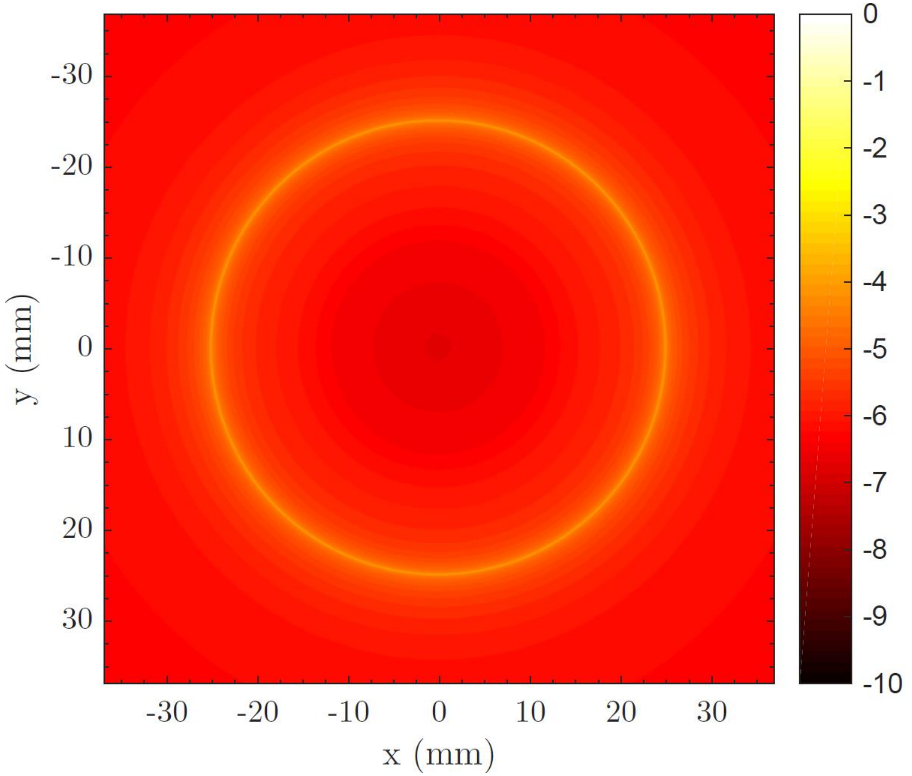

Propagation inside the coronagraph

- Intensity in plane C, with the Lyot stop

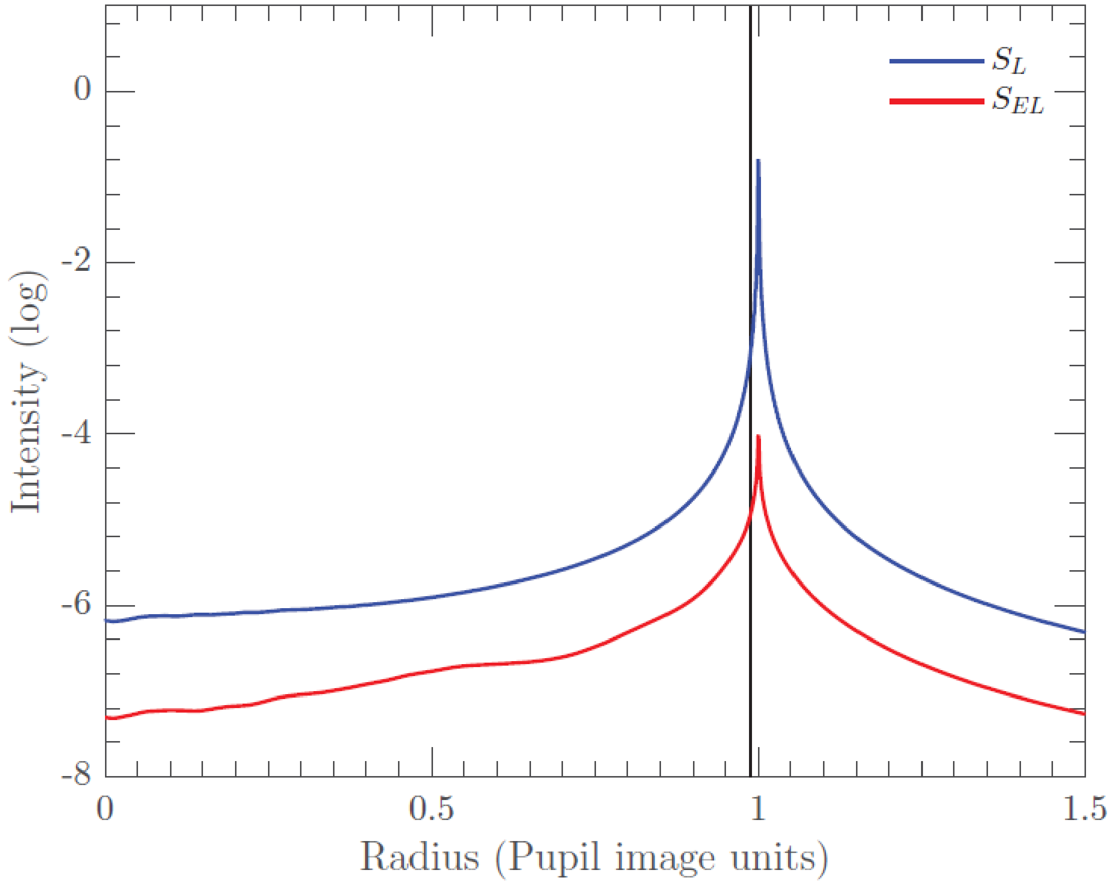

With external occulter

Without external occulter (Lyot coronagraph)

Propagation inside the coronagraph

- Intensity in plane C, with the Lyot stop

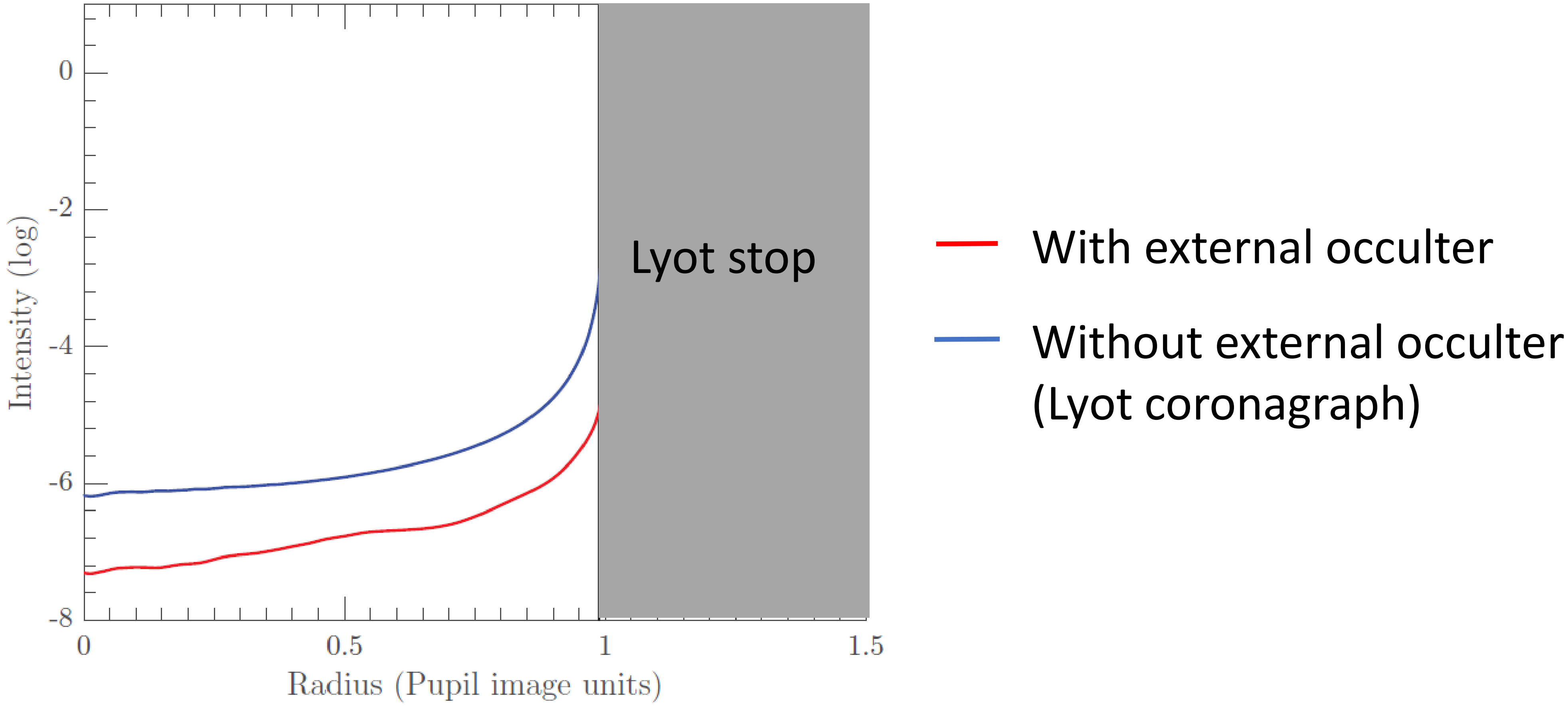

Propagation inside the coronagraph

- Intensity in plane D, final focal plane with the detector

With external occulter

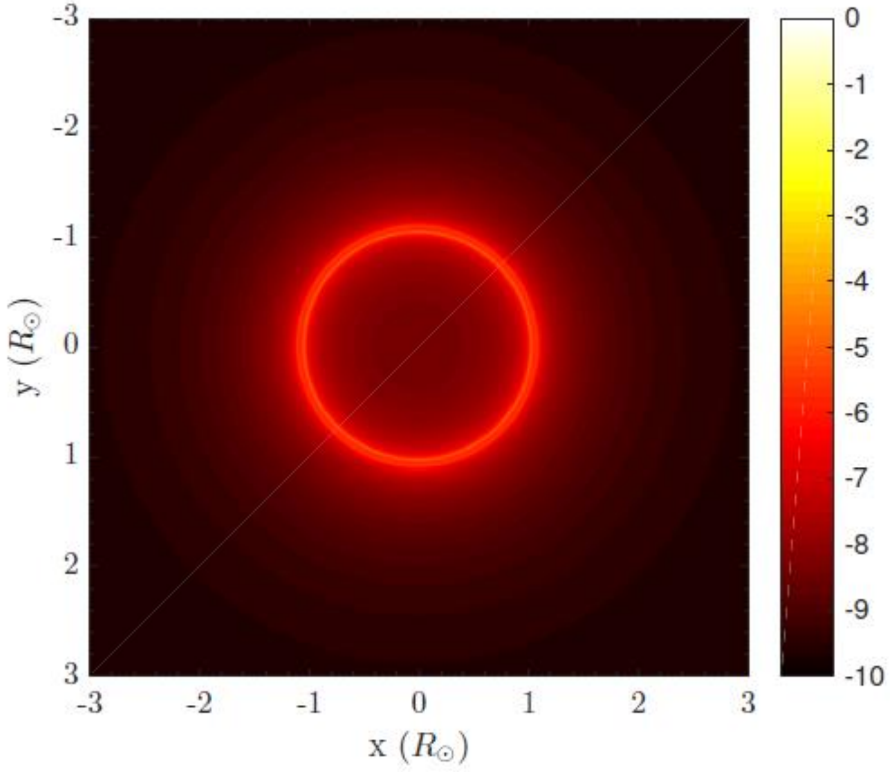

Propagation inside the coronagraph

- Intensity in plane D, final focal plane with the detector

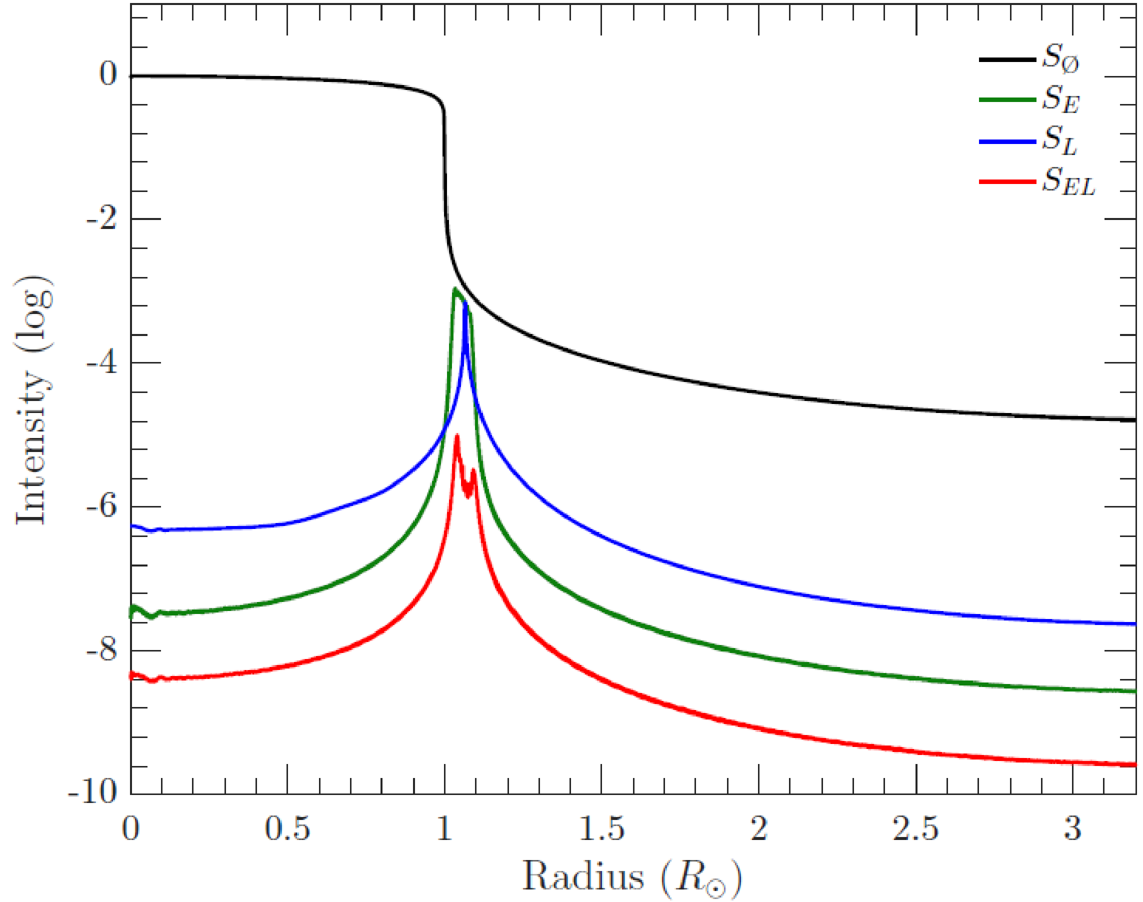

No occulter and stop
Solar disk image

Just the external occulter
No internal occulter
No Lyot stop

Without external occulter
(Lyot coronagraph)

With external/internal occulters and Lyot stop

Propagation inside the coronagraph

- Impact of sizing the internal occulter and the Lyot stop
  Intensity on plane D, the final focal plane

Fixed Lyot stop

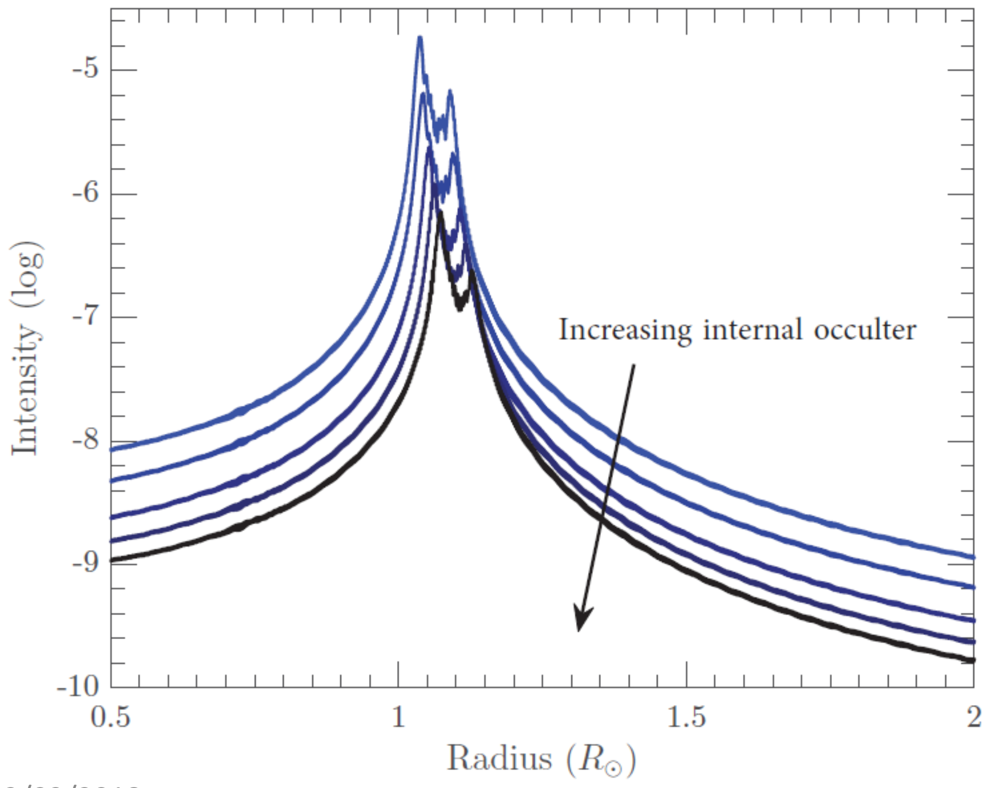

Fixed internal occulter

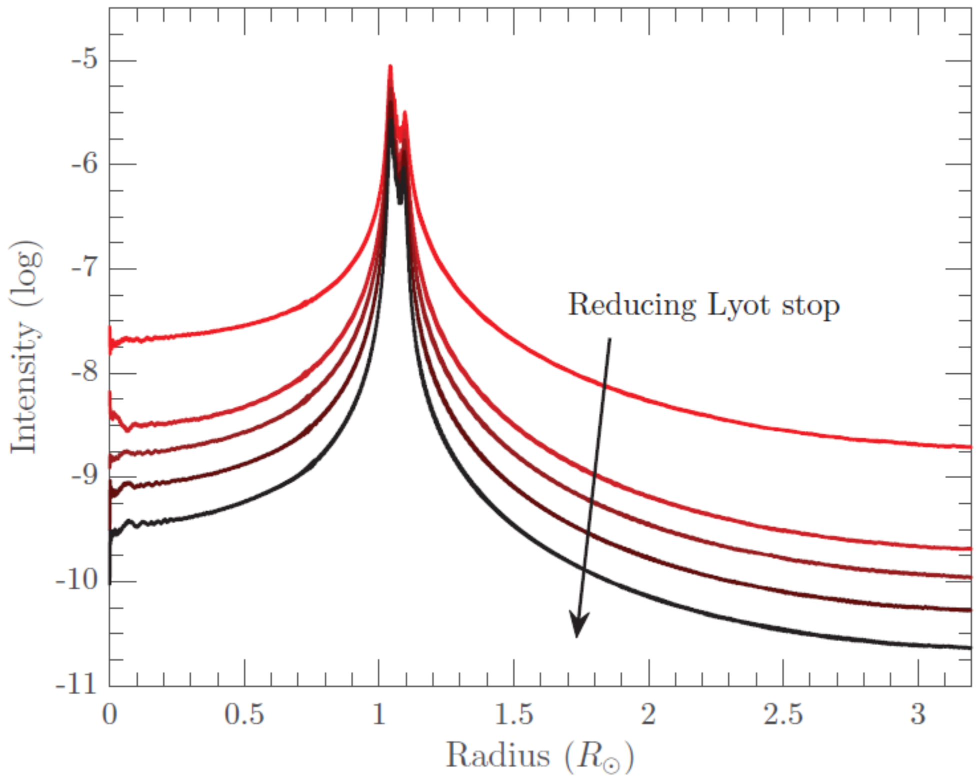

Propagation inside the coronagraph

- Impact of sizing the internal occulter and the Lyot stop

Residual diffracted sunlight @ $1.3R_\odot$

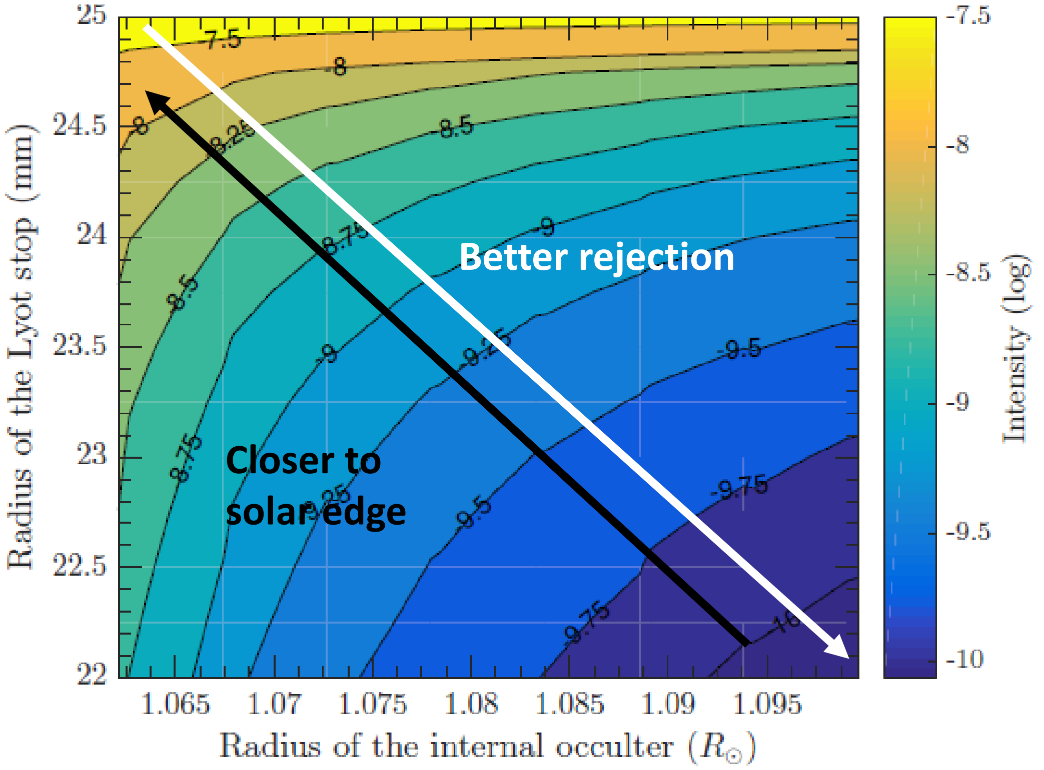

PSF in the vignetted zone

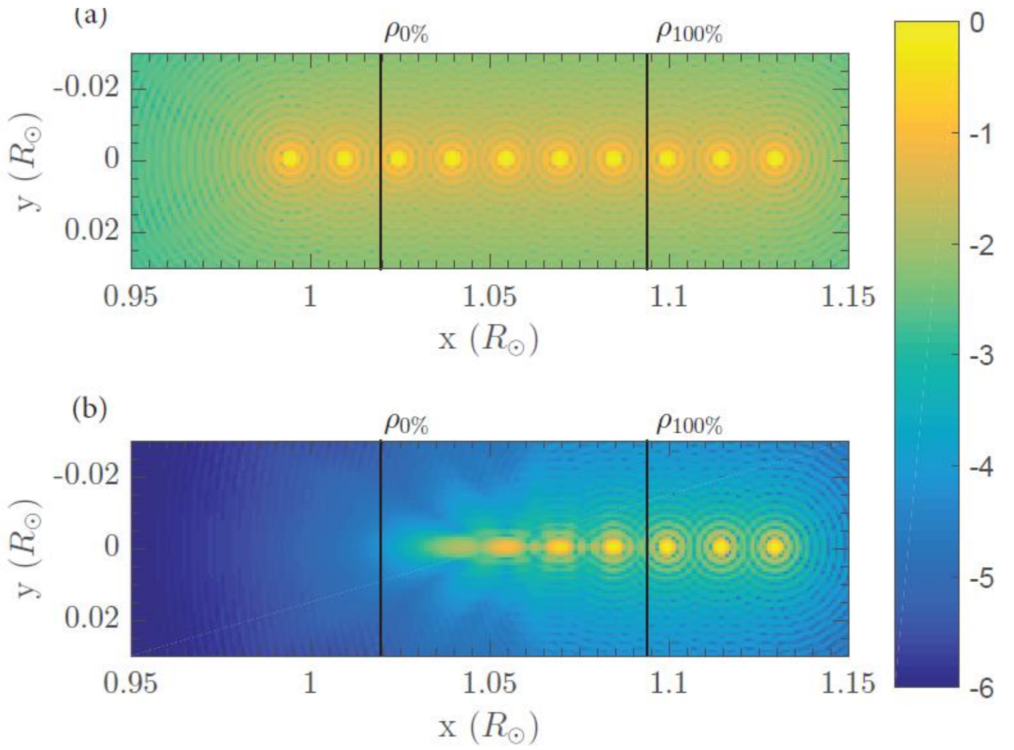

Conclusion

Conclusion

- Headlines of the presentation:
  - the different types of external occulter (in solar coronagraphy)
  - the penumbra profiles
  - propagation of diffracted light to understand rejection performance

- Reference:
  - Aime C., 2013, A&A
  - Rougeot R., Flamary R., Galano D., Aime C. 2017, A&A
  - Rougeot R., Aime C. 2018, A&A

Conclusion

- On-going/future works:
  - deviation from ideal optics: scattering, optical aberrations…
  - end-to-end performance for the serrated occulters

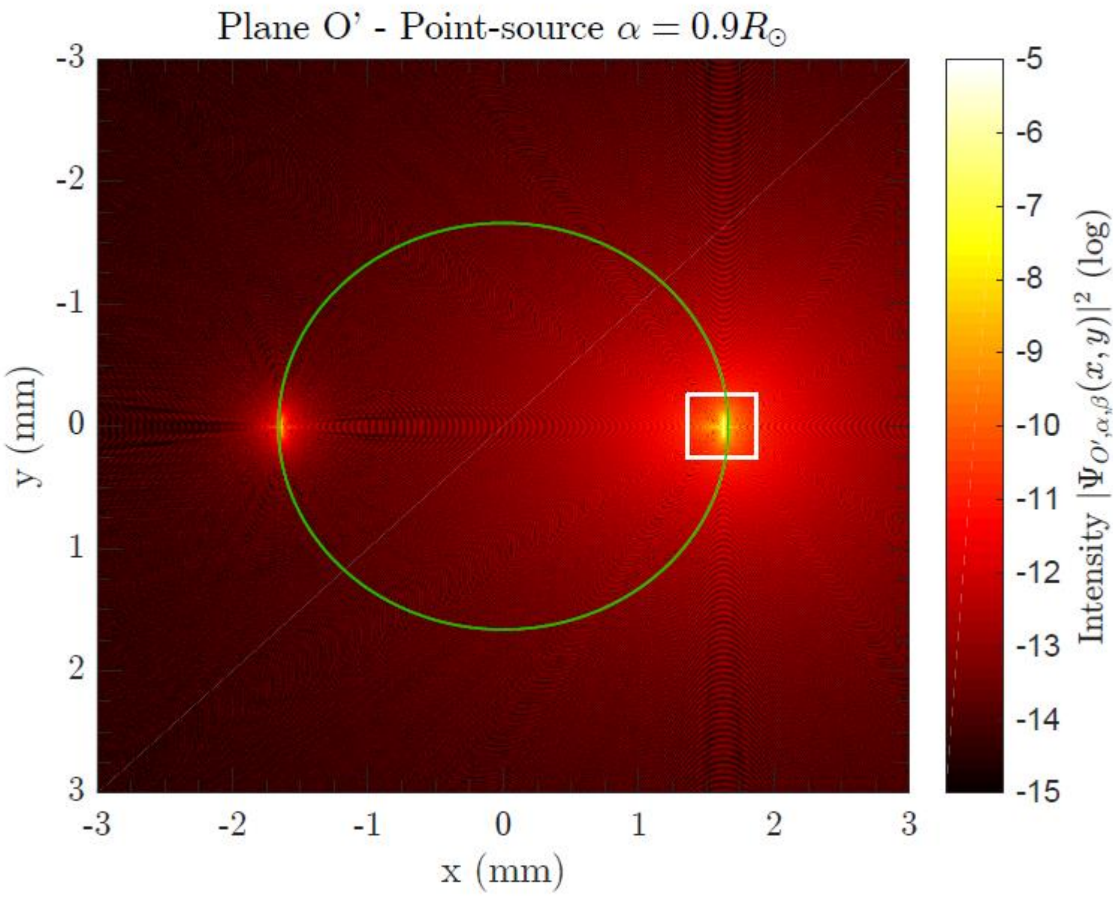

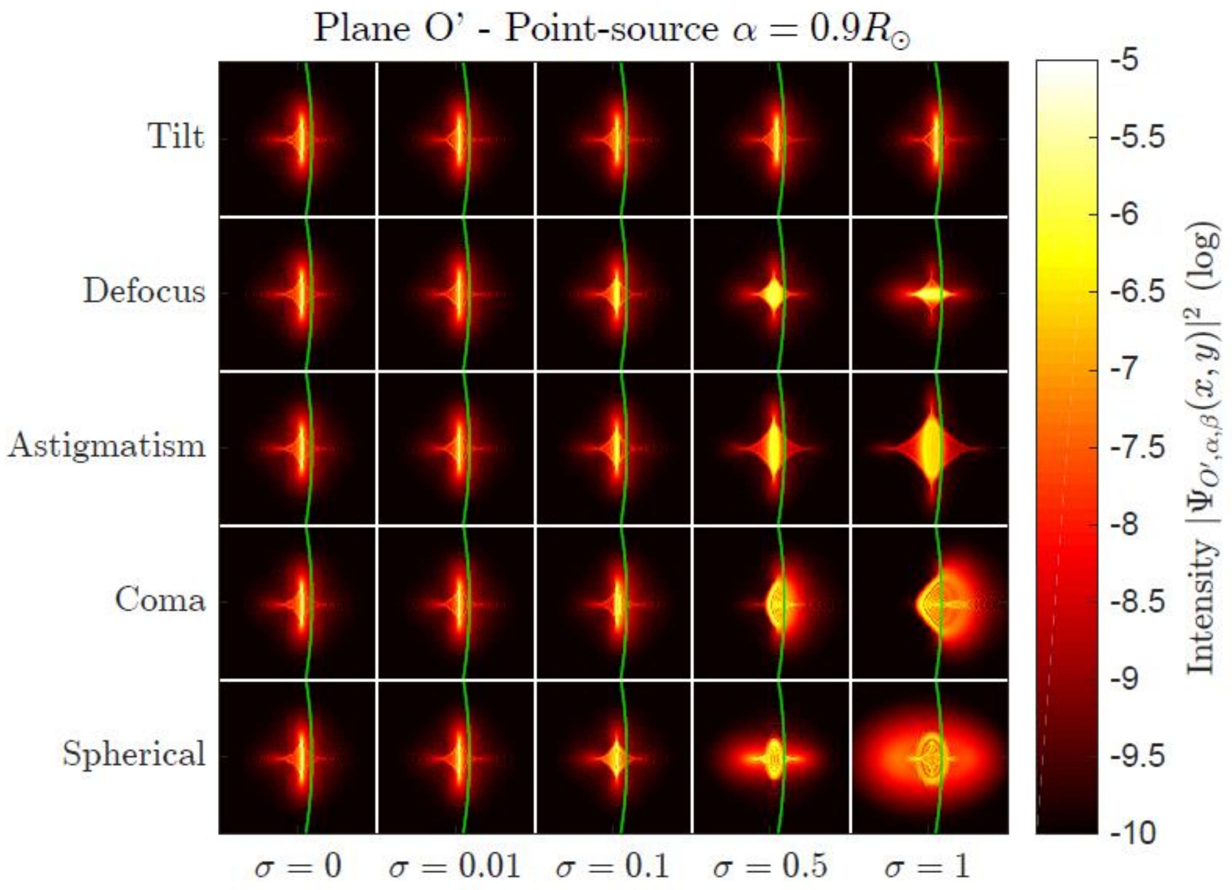

Questions?

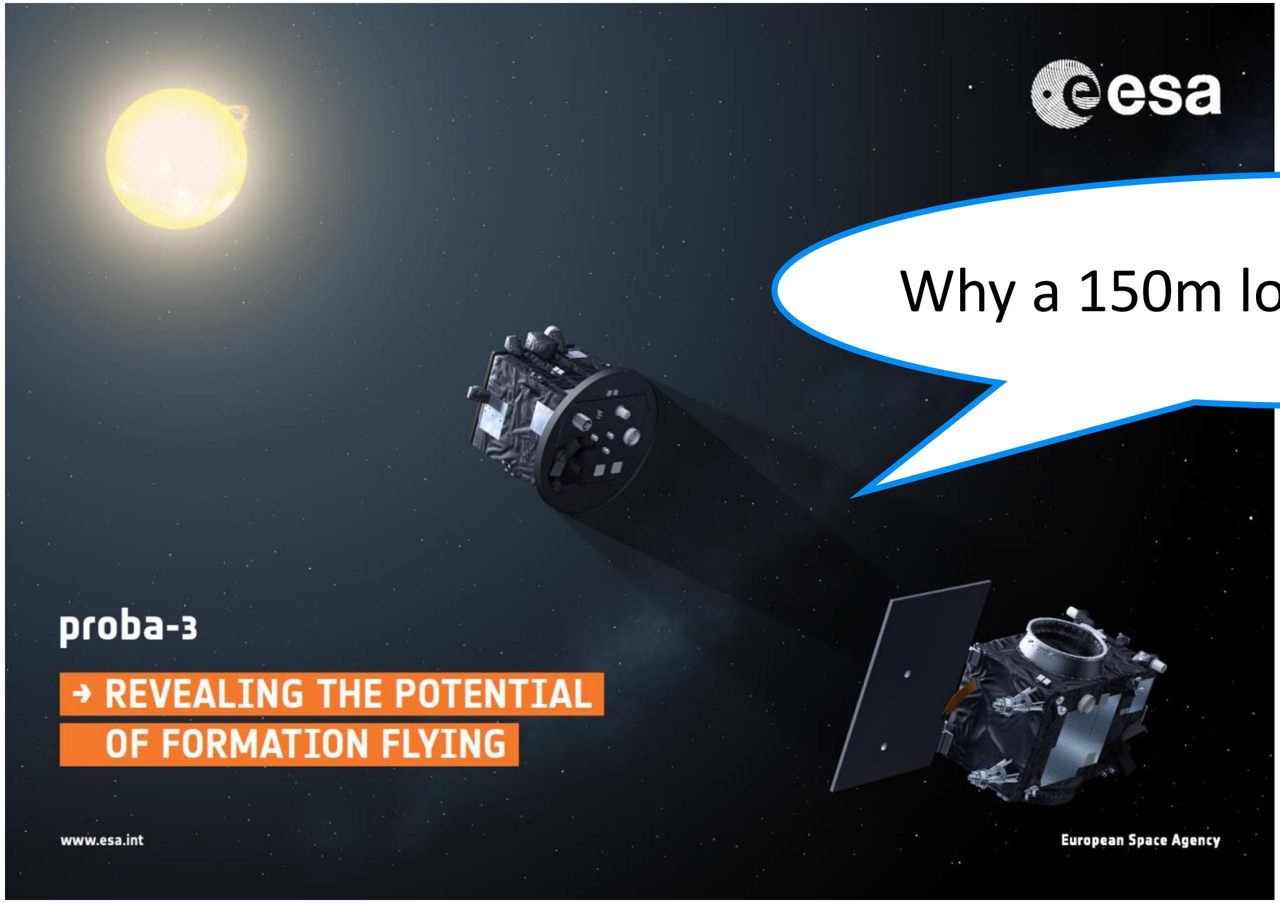

Why a 150m long coronagraph?

Thank you for your attention!

Annex

Diffraction by an external occulter

How to model diffraction? We looked at (when applicable):

	Radial apodisation	No axis-symmetry
Analytical Hankel transformation	√	X
Lommel series*	X	X
Vanderbei et al. (2017) approach**	√	√ (periodic)
Brute force 2D FFT	√	√
Rubinowicz representation	X	√

* Not introduced in this presentation

** Not suitable for the solar case

The Hankel transformation

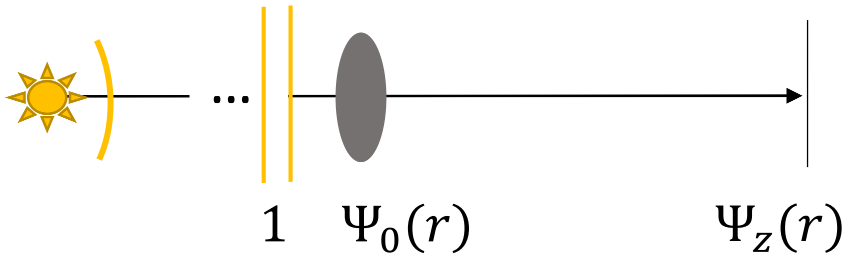

Fourier wave optics formalism

Fresnel free-space propagation

Axis-symmetric (apodized) occulter

$$\Psi_z(x,y) = \big(1 - f(r)\big) \circledast \frac{1}{i\lambda z} \exp\left(\frac{i\pi}{\lambda z}(x^2 + y^2)\right)$$

$$\Psi_z(r) = \frac{\varphi_z(r)}{i\lambda z} \int_0^R 2\pi\rho \times f(\rho) \times \exp\left(\frac{i\pi\rho^2}{\lambda z}\right) \times J_0\left(\frac{2\pi\rho r}{\lambda z}\right) d\rho$$

Diffraction at z
Radial function

Radial apodization

Lommel series – decomposition into series (Aime, 2013)

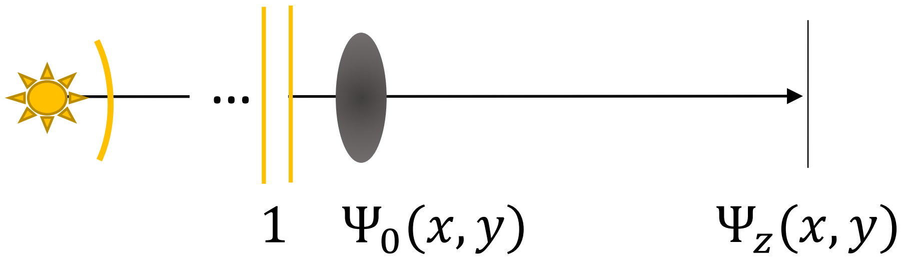

2D FFT technique

Fourier wave optics formalism

Fresnel free-space propagation

Occulter of any shape and any transmission (ideally)

$$\Psi_z(x, y) = \Psi_0(x, y) \circledast \frac{1}{i\lambda z} \exp\left(\frac{i\pi}{\lambda z}(x^2 + y^2)\right)$$

$$\Psi_z(x, y) = \mathcal{F}^{-1}\left[\mathcal{F}\left[\Psi_0(x, y)\right] \times \exp(-i\pi\lambda z(u^2 + v^2))\right]$$

Diffraction at z
2D function

Occulter
2D shape + apodisation

Fresnel filter

2D FFT technique

The occulter $\Psi_0(x, y)$ is padded in an array $K \times K$ with sampling σ

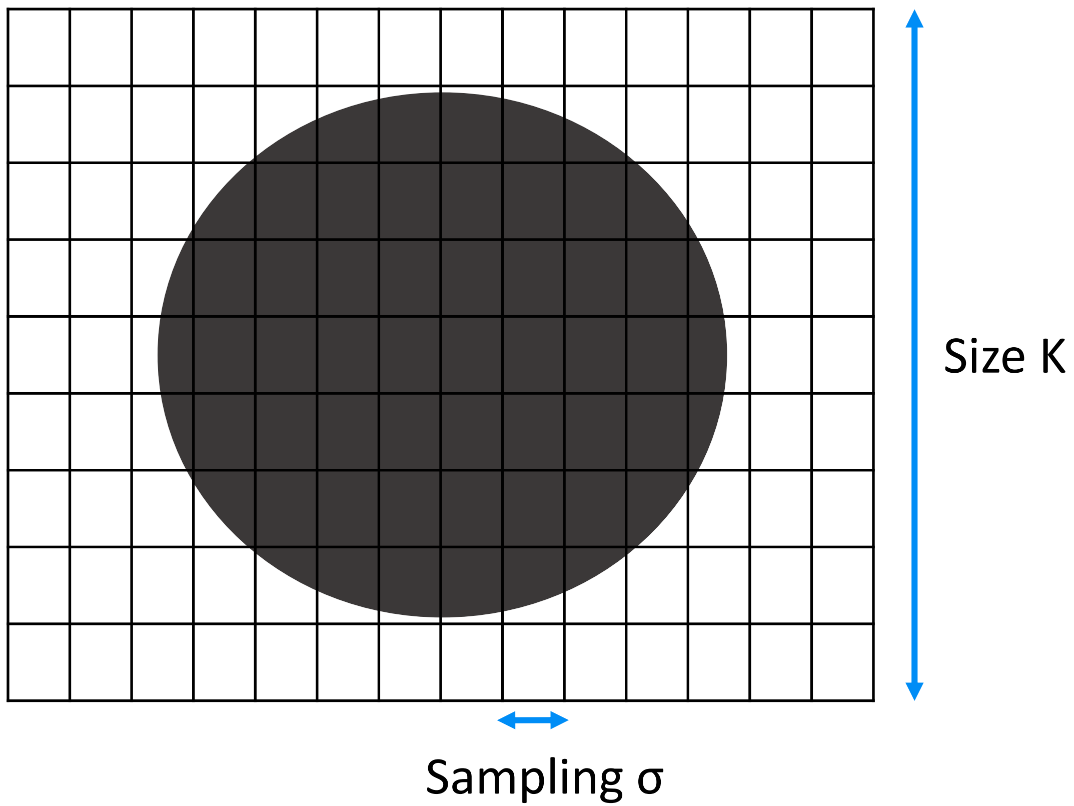

Usually, for FFT routines:

- The bigger K, the better (padding)

- The smaller σ, more accurate computation (high-frequency)

2D FFT technique

An additional condition!

The Fresnel filter $\exp(i\pi\lambda z u^2)$ has its phase varying as u^2

At the edge of the array, $u_c = 1/2\sigma$

We impose that the (maximum) phase variation at the edge of the array is $<\pi$

$$\sigma > \sqrt{\frac{\lambda z}{K}}$$

Consequence: $\sigma \searrow \Longrightarrow K \nearrow$

2D FFT technique

Very sensitive to numerical sampling: impact of the size of the array

2D FFT computation

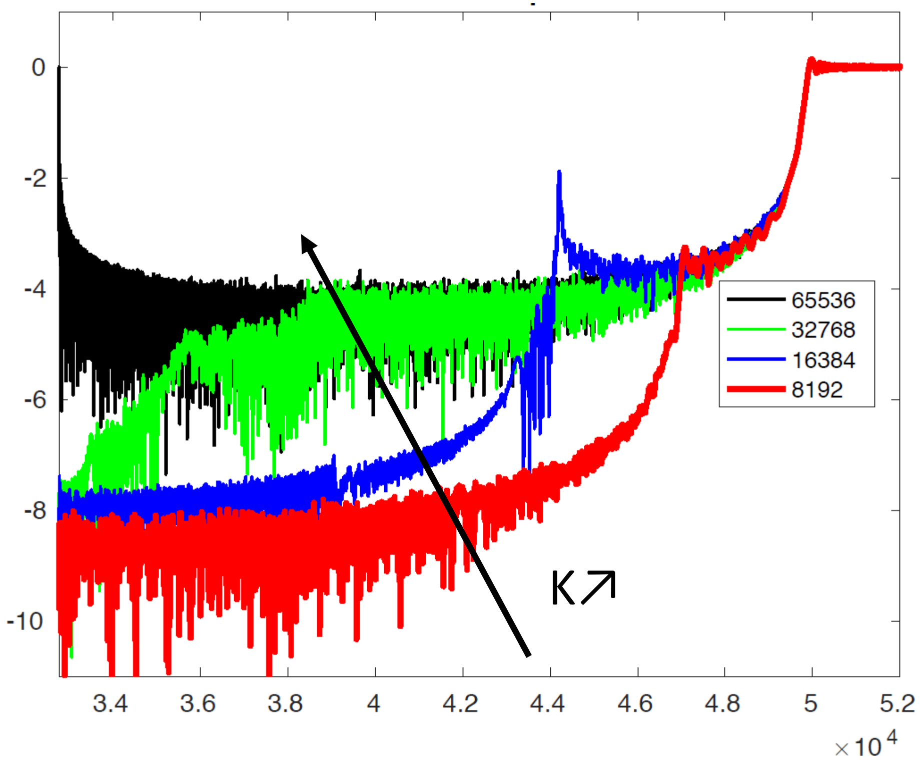

Reference curve (Hankel)

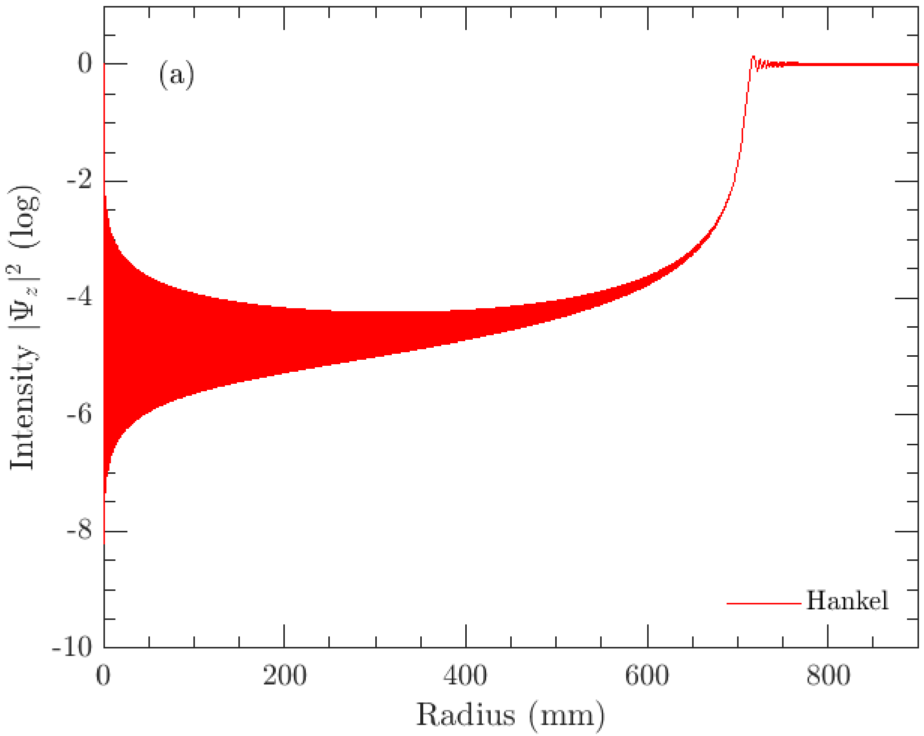

2D FFT technique

Very sensitive to numerical sampling: impact of sampling

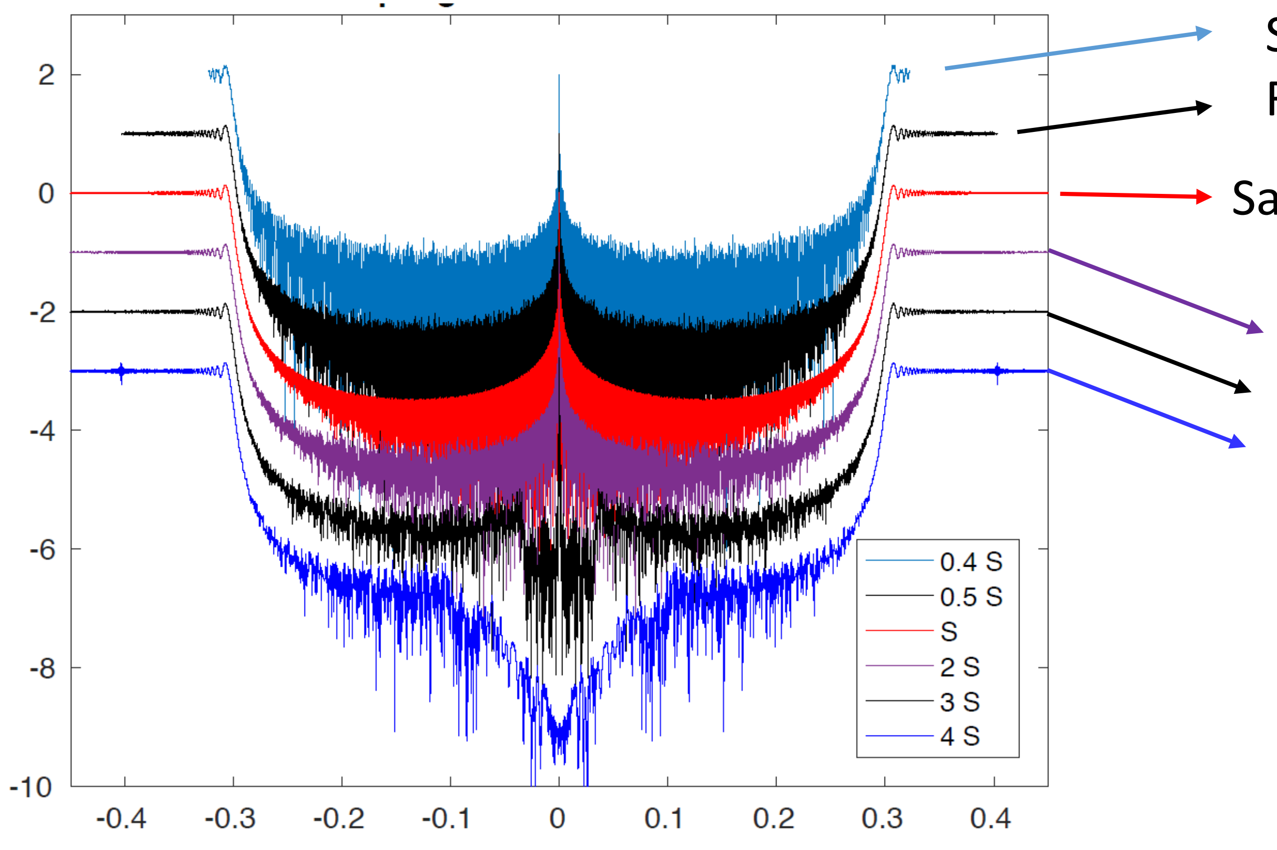

Sampling too small regarding Fresnel filter's condition

Sampling **S** meeting the condition

Sampling too large to correctly sample the occulter

Vanderbei et al.

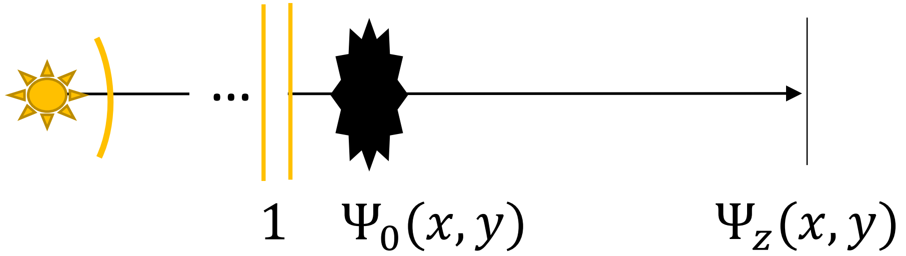

The use of serrated external occulters in stellar and solar coronagraphy comes from very different reasoning, but the diffraction principle is the same

Vanderbei et al. (2007) introduces another method to compute Fresnel diffraction
For serrated or petal-shaped occulter, i.e. a periodic pattern by rotation

$$\Psi_z(r,\theta) = \Psi_z^{apod}(r) + \sum_{j=1}^{\infty} f_1(j, N_t) \times \int_0^{R+\Delta} f_2(j,\rho) \times J_{jN_t}\left(\frac{2\pi r\rho}{\lambda z}\right)\rho d\rho$$

Diffraction from related apodized occulter

Sum up to infinity

High-orders Bessel functions (jN_t)

In stellar coronagraphy:
$N_t \approx 20$, and very small working angles: j=1 dominates

In solar coronagraphy:
$N_t \approx 100 - 1000$, and large region (671mm): the computation is very heavy

Rubinowicz representation

Based on Kirchhoff integral theorem (Born & Wolf ; Cady, 2012)

Requires a “1 or 0” occulter: no apodization

The diffraction is written as a boundary integral along the edge of the occulter

$$\Psi_z(x,y) = -\Psi_z^{(d)}(x,y) \text{ in the geometrical shadow}$$

$$\Psi_z(x,y) = \Psi_0 - \Psi_z^{(d)}(x,y) \text{ otherwise}$$

Geometrical wave: Ψ_0

Diffraction disturbance = boundary diffraction wave integral: $\Psi_z^{(d)}(x,y)$

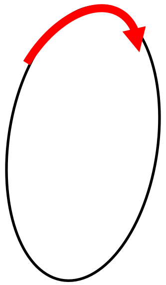

$$\Psi_z^{(d)} = \int_{\partial\Omega} W dl$$

Edge of the occulter

Penumbra for serrated occulters

Convolution of the diffraction intensity $|\Psi_z(x, y)|^2$ with the solar stenope image
Includes limb darkening function

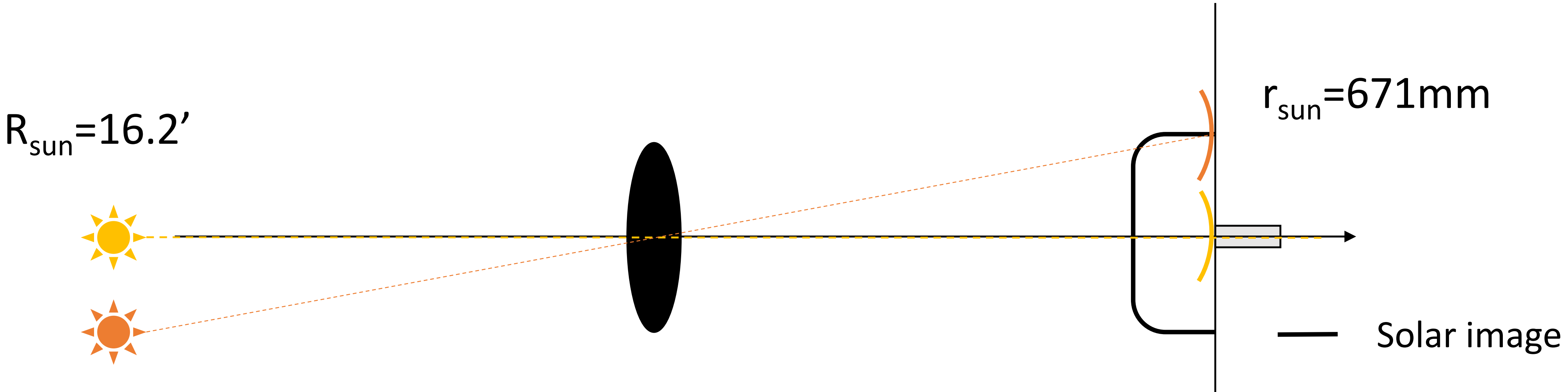

Penumbra: $\int_{☀}$ Diffraction x Solar image

Penumbra for serrated occulters

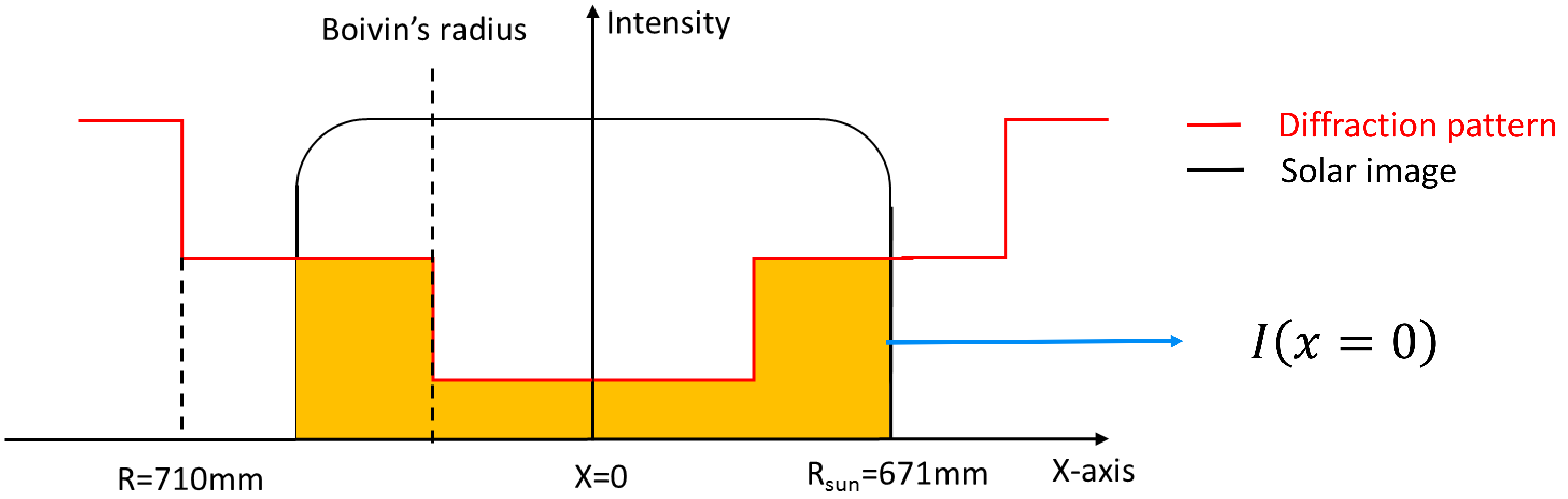

Penumbra for serrated occulters

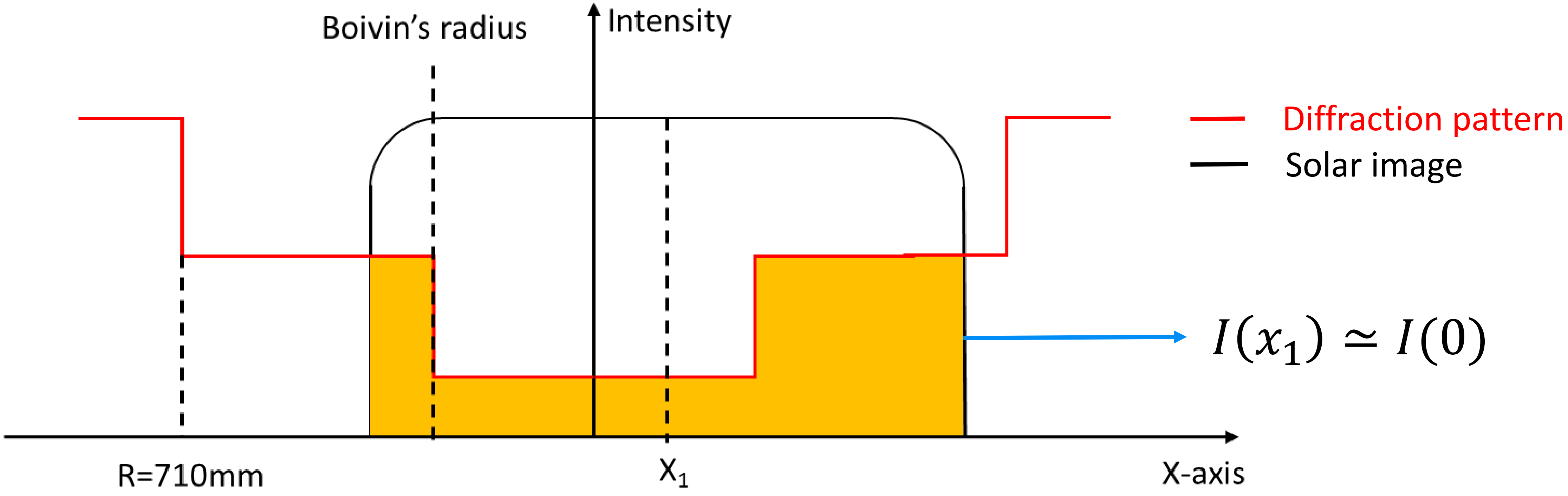

Penumbra for serrated occulters

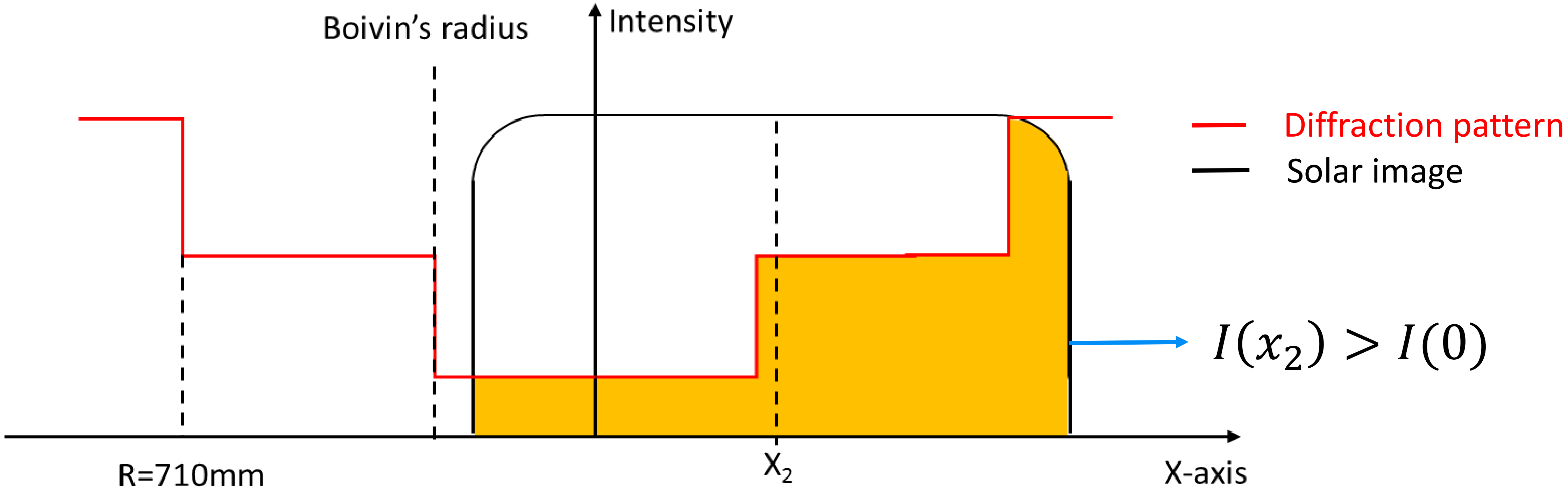

Penumbra for serrated occulters

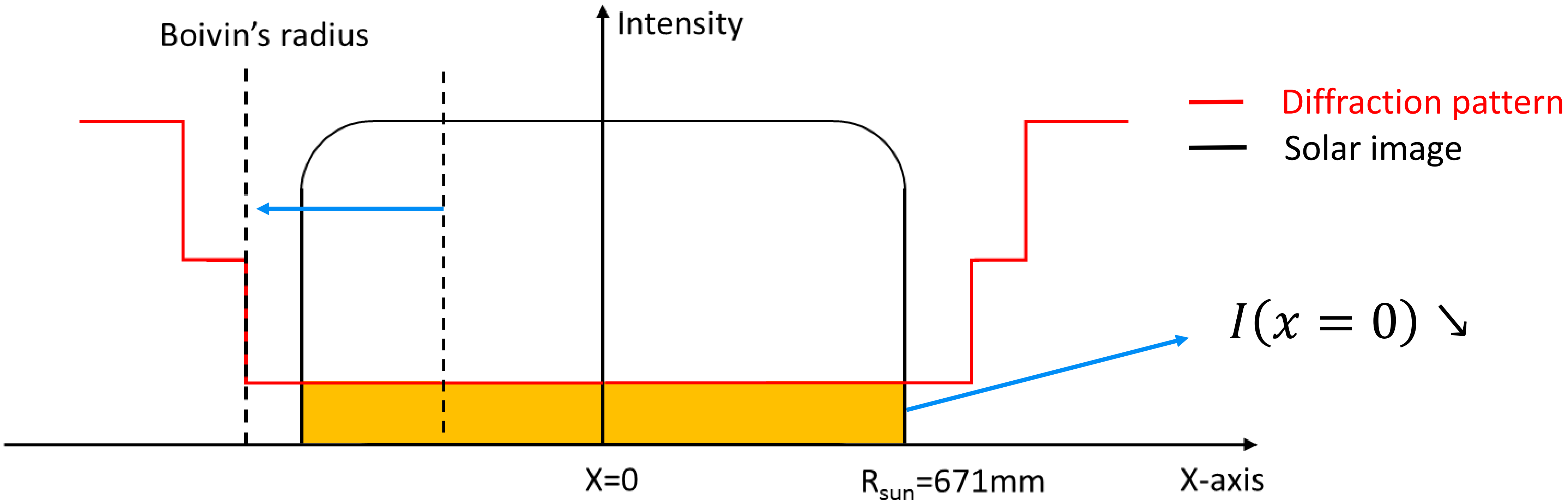

Penumbra for serrated occulters

We can predict the penumbra depth for serrated occulters:

The deepest umbra is achieved when:

$$\text{Boivin radius}(N_t, \Delta) > r_{sun}$$

The second parameter is the intensity level of the diffraction pattern

→ Large number of teeth preferred!